Inorganic Chemistry

Article

pubs.acs.org/IC

Nickel(II) and Palladium(II) Thiaethyneporphyrins. Intramolecular Metal(II)–η^2-CC Interaction inside a Porphyrinoid Frame

Elżbieta Nojman, Anna Berlicka, Ludmiła Szterenberg, and Lechosław Latos-Grażyński*

Department of Chemistry, University of Wrocław, 14 F. Joliot-Curie Street, 50-383 Wrocław, Poland

Supporting Information

ABSTRACT: 3,18-Diphenyl-8,13-di-*p*-tolyl-20-thiaethyneporphyrin ([18]thiatriphyrin(4.1.1)), which formally contains an C1−C2 ethyne moiety instead of pyrrole embedded in the macrocyclic framework of 21-thiaporphyrin, was obtained in a modification of the "3 + 1" approach using the ethyne analogue of tripyrrane (1,4-diphenyl-1,4-di(pyrrol-2-yl)but-2-yne) and 2,5-bis(*p*-tolylhydroxymethyl)thiophene. The spectroscopic and structural properties of 20-thiaethyneporphyrin reflect its macrocyclic aromaticity, revealing a combination of the acetylene (≥C−C≡C−C≤) and cumulene (>C═C═C═C<) character of the C18−C1−C2−C3 linker. The magnetic manifestations of aromaticity and antiaromaticity of thiaethyneporphyrin and its two-electron-oxidized derivative were observed using ^{1}H NMR spectroscopy and were confirmed by density functional theory calculations involving chemical shifts and nucleus-independent chemical shift analysis. Protonation of 20-thiaethyneporphyrin yielded a nonaromatic tautomer of *iso*-20-thiaethyneporphyrin, locating the saturated meso carbon adjacent to thiophene. Insertion of palladium(II) and nickel(II) into 20-thiaethyneporphyrin afforded planar palladium(II) thiaethyneporphyrin and low-spin diamagnetic nickel(II) 20-thiaethyneporphyrin as determined by X-ray crystallography. 20-Thiaethyneporphyrin acts as a dianionic ligand that coordinates through the two nitrogen and one sulfur donors. Metal(II) ions are uniquely exposed to form an intramolecular metal(II)–η^2-CC bond, whereas the organometallic fragment is coplanar with the whole macrocycle. Coordination of pyridine converts diamagnetic nickel(II) thiaethyneporphyrin into its paramagnetic counterpart as determined by ^{1}H NMR.

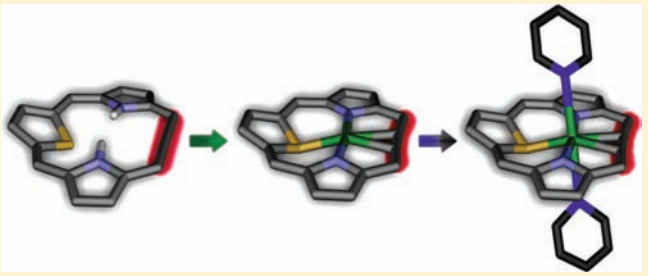

INTRODUCTION

Incorporation of an acetylene−cumulene unit into a porphyrinoid skeleton provides the unique means to design a molecular frame affording eventually effective control of the electronic structure that encloses the π-conjugation pathway of aromatic molecules. Originally, the annulene−cumulene moieties have been successfully embedded into porphyrinoids, heteroporphyrinoids, or expanded porphyrinoids, furnishing the specific subgroup of expanded porphyrinoids,[1−10] the representative examples of which include acetylene−cumulene porphycene **1** (Chart 1).[1]

Chart 1

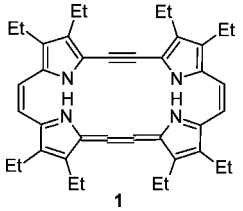

1

Exploration in this area can be motivated by the search for suitable chromophores potentially active at near-IR (NIR) because of the expanded π-conjugation pathway. Recently, we recognized that the concept of an acetylene−cummulene building block may be of importance in the construction of porphyrinoids derived formally from [14]triphyrins(n.1.1).[11,12]

Developments in the area of contracted porphyrinoids related to [14]triphyrins(1.1.1) (Chart 2), such as subphthalocyanine,[13] subporphyrazine,[14] subporphyrin,[15−17] and subpyriporphyrin **3**,[18] have been motivated by their potential applications in the fields of dyes, nonlinear optics, photonic devices, and materials sciences.[19−23] The recent progress is associated with the dynamically developing exploration of [*N*]triphyrins(*n*.1.1) including the seminal for the field of boron(III) [14]triphyrins(1.1.1) **2**.[15−17,24] Still, with the exception of subpyriporphyrin **3**, a homologue of [14]triphyrin(1.1.1) with a pyridine moiety embedded in the macrocyclic framework, all [14]triphyrins(1.1.1) were isolated as boron(III) complexes, which were typically applied as indispensable templating agents.[18,24] Preserving the fundamental features of subporphyrins, one can envisage the systematic modification of triphyrin(1.1.1), which requires elongation of the meso bridge (bridges). The replacement of nitrogen(s) by heteroatom(s) should also be considered. Accordingly, a group of aromatic β- and *meso*-substituted [14]triphyrins(2.1.1) and [14]benzotriphyrins(2.1.1) **4**, which are nearly planar metal-free contracted porphyrinoids, have recently been reported.[24−28]

Received: December 19, 2011
Published: February 22, 2012

   dx.doi.org/10.1021/ic2027175 | *Inorg. Chem.* 2012, 51, 3247−3260

Chart 2

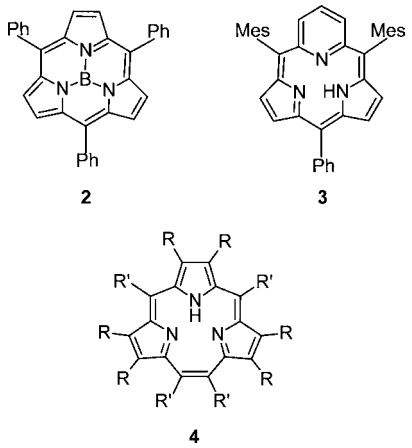

2 3 4

The replacement of the six inner protons of [18]annulene by three oxygen, sulfur, or NH(NR) groups or some combination of the three, as explored originally by Badger et al., leads to heteroatom-bridged annulenes related to [18]triphyrin(2.2.2).[29−31] Aza-deficient porphyrin 5,10,15,20-tetraaryl-21-vacataporphyrin [butadieneporphyrin or [18]triphyrin(6.1.1)], which is an annulene−porphyrin hybrid, can be also considered as a representative molecule for the whole subclass of homologous [*N*]triphyrins-(*n*.1.1).[32−34]

In the search for contracted porphyrinoids (heteroporphyrinoids) structurally related to putative [18]triphyrin(4.1.1), one can refer to two formal strategies where the final structure is being treated as derived from [14]triphyrin(1.1.1) or [18]porphyrin(1.1.1.1). Formally, [18]triphyrin(4.1.1) could be derived from [14]triphyrin(1.1.1) or [18]porphyrin(1.1.1.1) using the expansion (C_3 insertion) or replacement (pyrrole with −CC−) concepts.[35] Of course, in the present case, these hypothetical changes in the major skeleton must be accompanied by heteroatom(s) substitution and reduction.

Previously, we have probed such a strategy to obtain 19,21-dithiaethyneporphyrin (Chart 3) and, subsequently, the first contracted carbaporphyrinoid−dithiaethyneazuliporphyrin **6**.[11,12]

Chart 3

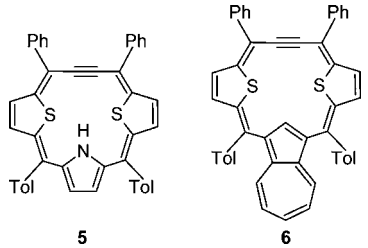

5 6

The coordinating abilities of **5** and **6** were exemplified by the formation of their ruthenium(II) complexes.

In the present work, we describe the synthesis and reactivity of a new porphyrinoid 20-thiaethyneporphyrin **7** (Chart 4), which, while 21-thiaporphyrin-like in character, is expected to have fundamentally different electronic and coordination properties. Eventually, the ability to coordinate nickel(II) and palladium(II), yielding the T-frame of coordinated metal(II) ions uniquely exposed to interact with the π CC bond, has been explored.

Chart 4

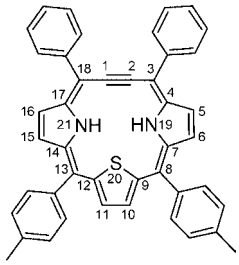

7

RESULTS AND DISCUSSION

Synthesis of 1,4-Di(phenyl-1,4-di(pyrrol-2-yl)but-2-yne (11). A key step in the synthesis of 3,18-diphenyl-8,13-di-*p*-tolyl-20-thiaethyneporphyrin **7** is the construction of **11**, which is a suitable synthon for introducing the ethyne unit into a porphyrin-like skeleton (Scheme 1).

Scheme 1. Synthesis of 11 (30%)[a]

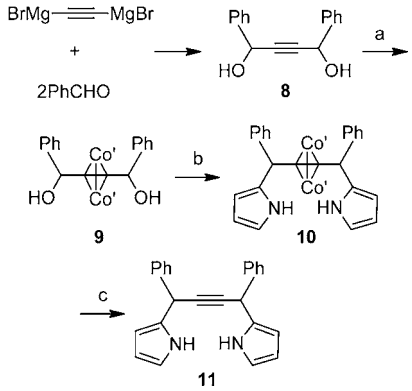

[a]Legend: (a) $Co_2(CO)_8$; (b) pyrrole, TFA; (c) $Fe(NO_3)_3{\cdot}9H_2O$; Co′ = $Co(CO)_3$.

1,4-Diphenyl-2-butyne-1,4-diol **8** has been obtained by applying the standard approach in the reaction of aryl aldehyde (benzaldehyde) with the Grignard reagent BrMgC≡CMgBr in tetrahydrofuran (THF).[36,37] Subsequently, the modified Nicholas reaction has been applied as shown in Scheme 1. The seemingly straightforward approach, i.e., a direct reaction between **8** and pyrrole (in excess) catalyzed with trifluoroacetic acid (TFA), failed to produce **11**. Complexation of an alkyne to dicobalt hexacarbonyl has been typically used to help stabilize the carbocationic charge generated at the carbon α to the alkyne moiety prior to treatment with a nucleophile. For instance, stable carbocationic intermediates that benefit from the β-effect of cobalt have been alkylated with several carbon nucleophiles to result in C−C bond formation.[38−44] Thus, **8** stirred with $Co_2(CO)_8$ in THF with the subsequent evolution of carbon monoxide gas afforded a stable dark-red complex **9** between the alkyne and dicobalt hexacarbonyl. Complex **9** was then treated with TFA to form a propargylic cation stabilized by the adjacent cobalt carbonyl moiety. The subsequent reaction with pyrrole as a nucleophile followed by decomplexation afforded a substituted alkyne **11** (yield 30%).

The molecular structure of **11** was determined by X-ray diffraction studies; the graphic representation is shown in Figure 1. The C2−C3 bond length [1.188(2) Å] reflects the

dx.doi.org/10.1021/ic2027175 | *Inorg. Chem.* 2012, 51, 3247−3260

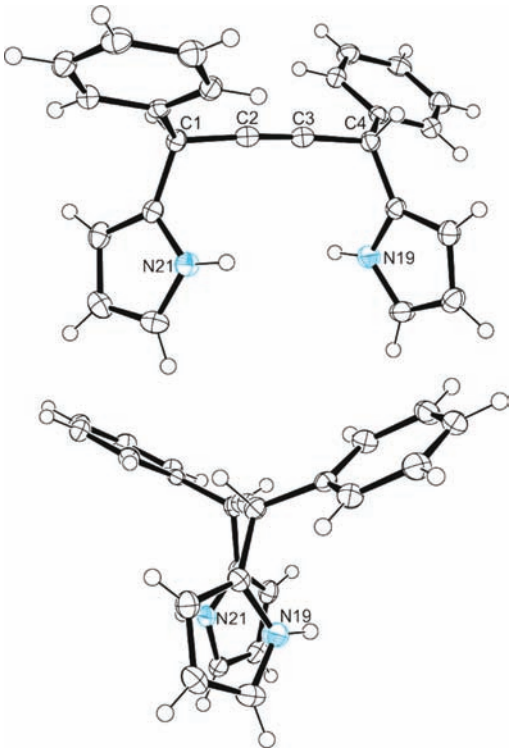

Figure 1. Molecular structure of **11** (top, perspective view; bottom, side view). The thermal ellipsoids represent 50% probability. Selected bond lengths: C1−C2, 1.478(2) Å; C2−C3, 1.188(2) Å; C3−C4, 1.483(2) Å.

ethyne structure of **11**. Accordingly, the characteristic ^{13}C resonance of ethyne (83.4 ppm) has been detected at ^{13}C NMR.

Synthesis and Characterization of 7. 20-Thiaethynephorphyrin 7 has been obtained in a simple modification of the "3 + 1" approach[10,45] described for *p*-benziporphyrin,[10,46,47] 24-thia-1,4-naphthiporphyrin,[10,48] expanded *p*-benziporphyrins[48,49] and heterocarbaporphyrins[11,48−50] using the ethyne analogue of tripyrrane **11** (Scheme 2).

Scheme 2. Synthesis of 7 (33%)[a]

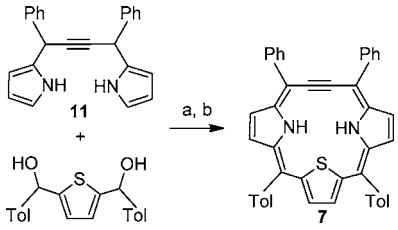

[a]Legend: (a) BF_3:OEt_2; (b) Et_3N, DDQ.

The electronic spectrum of 7 (Figure 2) demonstrates a distinct intense Soret-like band at 439 nm accompanied by less intense Q bands at 508, 539, 630, and 710 nm, resembling the spectroscopic features of aromatic 5,10,15,20-tetraphenyl-21-thiaporphyrin.[51]

The ^1H NMR spectrum of 7 presents resonances at positions consistent with an aromatic structure and resembles that of 21-thiaporphyrin (Figure 3, trace A).[51] Assignments of the ^1H and ^{13}C NMR resonances for 7 have been made on the basis of relative intensities and detailed two-dimensional NMR experiments (COSY, NOESY, HSQC, and HMBC). The molecule 7

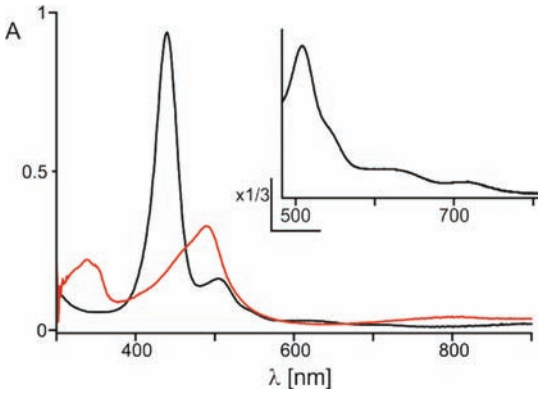

Figure 2. UV−vis absorption spectra (298 K, CH_2Cl_2) of 7 (black line) and $[\mathbf{13}\text{-}H_2]^{2+}$ (red line). Inset: Q bands of 7.

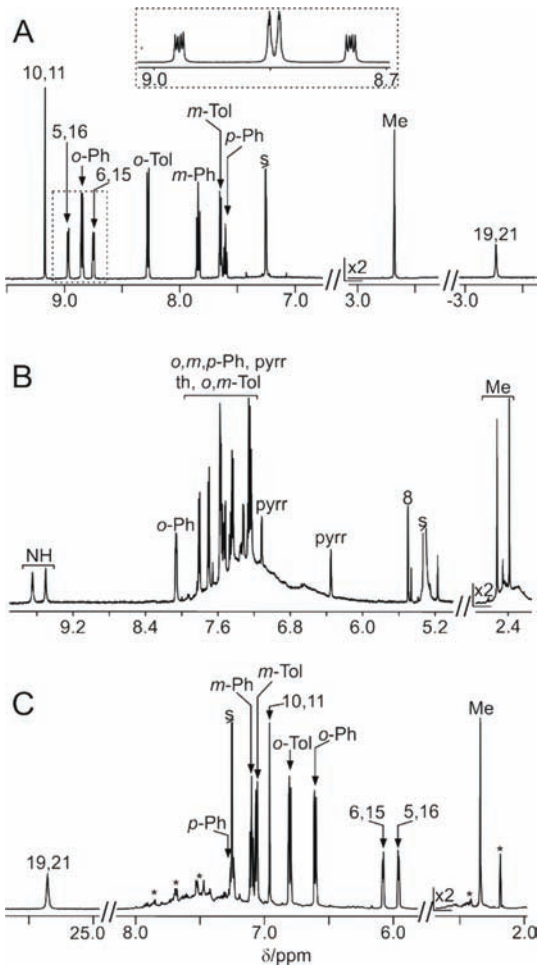

Figure 3. ^1H NMR spectra of (A) 7 ($CDCl_3$, 300 K), (B) **12**′-H^+ (CD_2Cl_2, 300 K), and (C) $[\mathbf{13}\text{-}H_2]^{2+}$ ($CDCl_3$, 300 K). Peak labels follow systematic position numbering or denote proton groups: *o*-, *m*-, *p*-Ph are the ortho, meta, and para positions of the *meso*-aryl groups. Inset: pyrrole region of 7. Resonance assignments at trace B: pyrr, pyrrole; th, thiophene. The broad resonance centered at 7.5 ppm in traces B and C is tentatively assigned to the unidentified products of oxidation.

retains the macrocyclic aromaticity, reflecting the presence of an 18-π-electron delocalization pathway. The scalar coupling detected between 19,21-NHs and β-pyrrolic hydrogen atoms confirms the molecular structure of 7.

dx.doi.org/10.1021/ic2027175 | *Inorg. Chem.* 2012, 51, 3247−3260

The ^{13}C chemical shifts of a four-carbon linker derived from 2-butyne are equal to 117.9 ppm for C1 and C2 and 102.3 ppm for C3 and C18. Two canonical structures of **7** define 18-π-electron macrocyclic delocalization pathways (Scheme 3). The

Scheme 3. Canonical Structures of 7

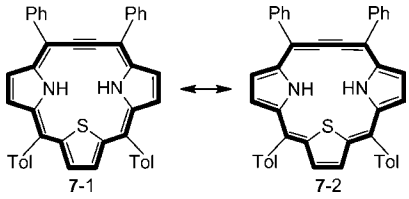

cumulene segment itself of 7-2 contributes four π electrons (rather than six) because of the perpendicular orientation of the p orbitals that make up the central π bond.

Accordingly, the electronic structure of **7** can be described as reflecting a combination of the acetylene (≥C−C≡C−C≤) and cumulene (>C═C═C═C<) character of the C18−C1−C2−C3 fragment. The relevant chemical shift values of acetylene or cumulene carbon atoms adjacent to aryl or 2-thienyl moieties have been considered in comparisons. The C_{sp} carbon atoms of **11** produces a ^{13}C NMR resonance at 83.4 ppm, in the 70−95 ppm range typical for acetylene. The ^{13}C NMR chemical shifts of cumulene fragments vary in the relatively wide range: 140.53 ppm for tetra(2-thienyl)butatriene,[52] 152.03 ppm for tetraphenylbutatriene,[53] and 134.48 ppm for 6,7,18,19-tetradehydrotetrathia[24]annulene(4.0.4.0), where, however, some admixture of the acetylenic structure was suggested.[4] Thus, the ^{13}C NMR chemical shifts of **7** point out that 7-1 and 7-2 contribute to the overall electronic structure, although the cumulenic character of the C18−C1−C2−C3 moiety prevails. The detected chemical shifts of **7** are fairly typical for acetylene−cumulene porphyrinoids[1,2,53] and acetylene−cumulene annulenes[54] and resemble that determined for 19,21-dithiaethyneporphyrin **5**.[11]

The molecular structure of **7**, determined in a X-ray diffraction study, is shown in Figure 4. The $C_{sp^2}C_{sp}C_{sp}C_{sp^2}$ butyne moiety is practically linear [C18−C1−C2, 178.5(1)°; C1−C2−C3, 179.2(2)°]. In comparison to **11**, which can be considered here as a standard acetylene-like reference, the statistically significant shortening of the C18−C1/C2−C3 (0.10 Å) bond distance and elongation of the C1−C2 (0.05 Å) bond distance have been detected. This observation firmly reflects the essential role of cumulene contributor 7-2 in the description of 20-thiaethyneporphyrin.

The bond distances within the framework of **7** indicate that the macrocycle reveals the bond-length pattern expected for aromatic porphyrinoids.[10,55] In particular, the C18−C1 and C2−C3 distances [1.380(2) and 1.385(2) Å] approach the aromatic bond limit. The aromaticity of **7** is clearly demonstrated by equalization of the $C_\alpha-C_{meso}$ bond lengths [C2−C3, 1.385(2) Å; C3−C4, 1.420(2) Å; C7−C8, 1.428(2) Å; C8−C9, 1.402(2) Å]. There is an appreciable effect of the conjugation on the thiophene fragment. The bond lengths within the thiophene ring are altered. Thus, the $C_\alpha-C_\beta$ bonds in **7** [1.421(2) and 1.418(2) Å] are longer than the $C_\beta-C_\beta$ distances [1.377(2) Å], whereas the reverse is true for tetrathiaporphyrinogen.[56]

Formation of *iso*-Thiaethyneporphyrin. The addition of an appropriate electrophile to the evidently electron-rich **7** has

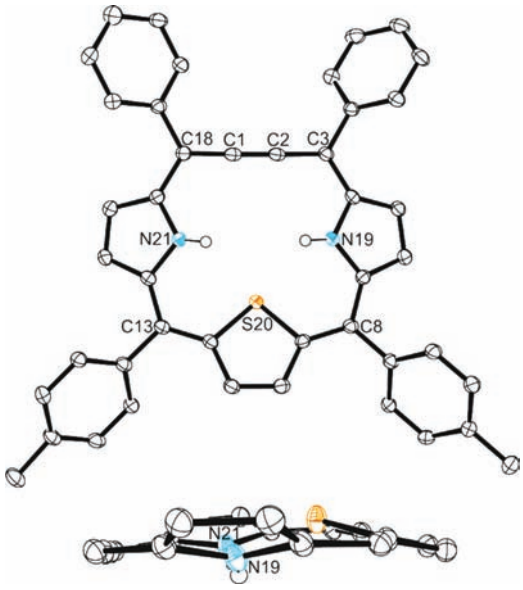

Figure 4. Molecular structure of **7** (top: perspective view; bottom: side view with aryl groups omitted for clarity). The vibrational elipsoids represent 50% probability. The bond lengths in the $C_{sp^2}C_{sp}C_{sp}C_{sp^2}$ (C18−C1−C2−C3) unit are 1.380(2), 1.238(2), and 1.385(2) Å. The dihedral angles between the plane of four *meso*-carbon atoms (C3, C8, C13, and C18) and the planes of five-membered rings are as follows: pyrrole 18.3°, thiophene 16.5°, and pyrrole 16.1°.

been considered as a feasible route to generating novel macrocyclic forms. Thus, titration of **7** with HBF_4 etherate or TFA has been carried out in dichloromethane-d_2 (298 K). The progress of this reaction has been systematically monitored by ^1H NMR. Judging by the ^1H NMR spectra of the reaction mixture, the process is quite complex. In the conditions of the experiment, the protonation is not reversible. The transient species **12**′-H readily undergoes unexplored degradation, yielding the broad peak centered at 7.5 ppm (Figure 3, trace B). Still, the positions of the narrow resonances including the NH ones reflect the structural features of **12**′-H^+ shown in Scheme 4.

Scheme 4. Protonation of 7

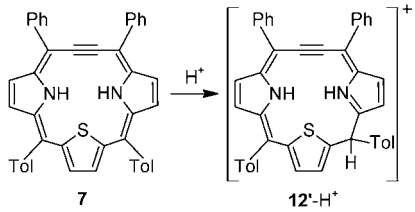

The ^1H NMR resonances of **12**′-H^+ were detected in the region that is typical for the conjugated but nonaromatic system.[11,57,57,58] The ^1H NMR chemical shift of H8 equals 5.5 ppm and is consistent with tetrahedral hybridization around the adjacent *meso*-carbon.[58] In the COSY map, this resonance revealed the scalar coupling to the thiophene H10, which allowed the unambiguous determination of the protonation site. Actually, a macrocyclic structural motif present at **12**′-H^+ can be identified as one of two nonaromatic **12**′ and **12**″ tautomers of *iso*-thiaethyneporphyrins with a saturated *meso*-carbon, shown schematically in Chart 5.

dx.doi.org/10.1021/ic2027175 | *Inorg. Chem.* 2012, 51, 3247−3260

Chart 5. Hypothetical *iso*-Thiaethyneporphyrins

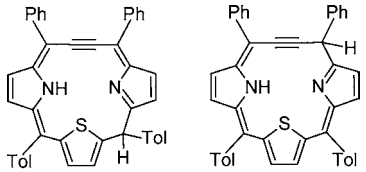

Oxidation of 7. Cyclic voltammetry (Figure S6 in the Supporting Information) demonstrates that **7** undergoes two consecutive, reversible one-electron oxidations with semireversible half-wave potentials (1) −74 mV and (2) +202 mV (if the half-wave potential of ferrocene equals 0 mV), yielding $\mathbf{7}^{\bullet+}$ and $[\mathbf{13}\text{-}H_2]^{2+}$, respectively (Scheme 5). These potentials are very low, which accounts for the easy accessibility of the oxidized forms.

Scheme 5. Oxidation of 7

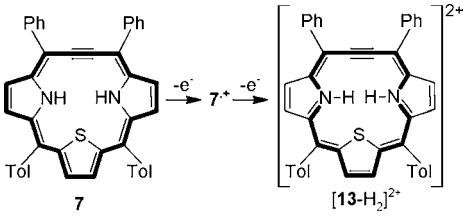

Oxidation of **7** in chloroform-*d* or dichloromethane-d_2 with varying amounts of 2,3-dichloro-5,6-dicyano-*p*-benzoquinone (DDQ) has been followed by ^{1}H NMR. In fact, the addition of DDQ resulted in extreme broadening of all resonances practically beyond detection. Presumably, the presence of even a minute amount of the radical $\mathbf{7}^{\bullet+}$ leads to significant line broadening and shortening of the T_1 relaxation times, confirming fast electron exchange between differently oxidized forms of **7**.[59] Finally, in this condition oxidation resulted in the irreversible degradation of **7**. The analogous oxidation of **7** with DDQ in chloroform-*d* or dichloromethane-d_2 but in the presence of HBF_4 afforded a well-resolved ^{1}H NMR spectrum readily assigned to $[\mathbf{13}\text{-}H_2]^{2+}$, the diprotonated form of [16]thiaethyneporphyrin (Figure 3, trace C). During oxidation, the color of the solution changes from orange to brown-red. The UV-Vis electronic spectrum (Figure 2) presents the features assigned to antiaromaticity. The ^{1}H chemical shifts observed for $[\mathbf{13}\text{-}H_2]^{2+}$, in particular the peculiar upfield position of the inner H19 and H21 hydrogen atoms (25.35 ppm), show that a paratropic ring current is present in the macrocycle (Figure 3, trace C). The antiaromatic behavior is also reflected by the reverse order of *meso*-aryl resonances (*p*-H > *m*-H > *o*-H).[33] In particular, the upfield relocation of the ortho protons (phenyl 6.6, *p*-tolyl 6.8 ppm) seems to be of significance. The pyrrolic *β*-H signals of $[\mathbf{13}\text{-}H_2]^{2+}$ at 5.96 and 6.08 ppm are slightly shifted upfield relative to the nonaromatic fully conjugated systems, which contain pyrrole moieties.[57,60] The resonances of $[\mathbf{13}\text{-}H_2]^{2+}$ disappeared after the addition of pyridine-d_5 to the NMR sample. The addition of HBF_4 resulted in the recovery of $[\mathbf{13}\text{-}H_2]^{2+}$.

Formation and Characterization of Palladium(II) and Nickel(II) Complexes. Palladium(II) and nickel(II) have been inserted into thiaethyneporphyrin to give formally four-coordinated complexes of palladium(II) thiaethyneporphyrin **7**-Pd and low-spin diamagnetic nickel(II) thiaethyneporphyrin (Scheme 6). The 20-thiaethyneporphyrin **7** acts as a dianionic

Scheme 6. Insertion of Metal(II) to Thiaethyneporphyrin 7[a]

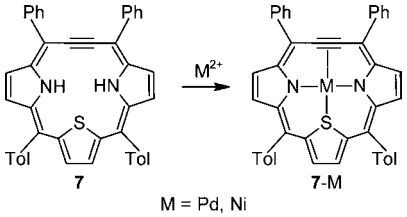

[a]Reaction conditions: 7-Pd, $Pd(OAc)_2$ (10 equiv), toluene, reflux, 4 h, 60%; 7-Ni, $Ni(OAc)_2{\cdot}4H_2O$ (10 equiv), toluene, reflux, 5 h, 50%.

ligand coordinating through the two nitrogen and one sulfur donors. To complete the coordination sphere of metal, interaction with the ethyne moiety is required (*vide infra*).

7-Pd is stable in solution and can be chromatographed. Solutions of **7**-Ni undergo gradual demetalation to give free thiaethyneporphyrin **7**. Originally, the identity of **7**-M was confirmed by high-resolution mass spectrometry (HR-MS) and NMR spectroscopy. The electronic absorption spectra of **7**-Pd and **7**-Ni are presented in Figure 5. These complexes have

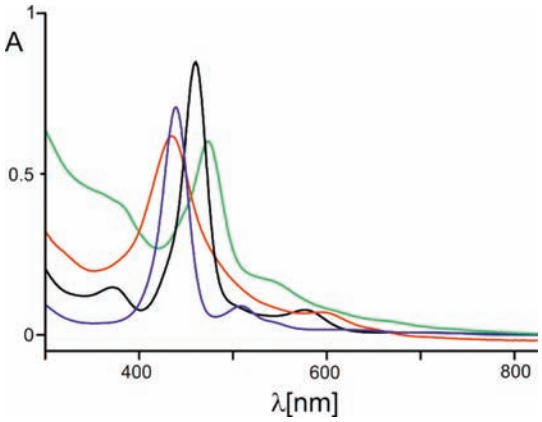

Figure 5. UV−vis absorption spectra (298 K, CH_2Cl_2) of **7** (blue line), **7**-Pd (black line), **7**-Ni (red line), and **14**-Pd (green line).

spectral characteristics that resemble those of thiaethyneporphyrin. The marked bathochromic shift of the Soret-like band has been determined for **7**-Pd.

7-Pd and **7**-Ni have effective C_s symmetry, with the mirror plane passing through the metal ion, thiophene sulfur, and the center of the C1−C2 bond. As a consequence, the representative ^{1}H NMR spectrum of **7**-Pd (Figure 6, trace A) contains the AB pattern of pyrrole resonances accompanied by the thiophene singlet resembling closely the ^{1}H NMR spectrum of **7**. The insertion of palladium resulted also in rather modest changes in the ^{13}C chemical shift. The ^{13}C chemical shifts of a four-carbon linker derived from 2-butyne are equal to 115.8 ppm for C1 and C2 and 107.2 ppm for C3 and C18 and are practically identical with those for the free base **7**. Nonequivalence of two macrocyclic sides due to the side-on coordination of the thiophene of **7**-M causes each aryl ring to have two distinct ortho and two meta resonances, unless the rotation around the $C_{meso}-C_{ipso}$ bond is sufficiently fast. Significantly, *meso*-tolyls of **7**-Pd, flanking the thiophene unit, demonstrate two *o*-H resonances typical for the slow rotation limit even at 300 K. At same time, the averaged features of *meso*-phenyl resonances have been seen. As the temperature is lowered, these meta and ortho resonances are splitting because

dx.doi.org/10.1021/ic2027175 | Inorg. Chem. 2012, 51, 3247−3260

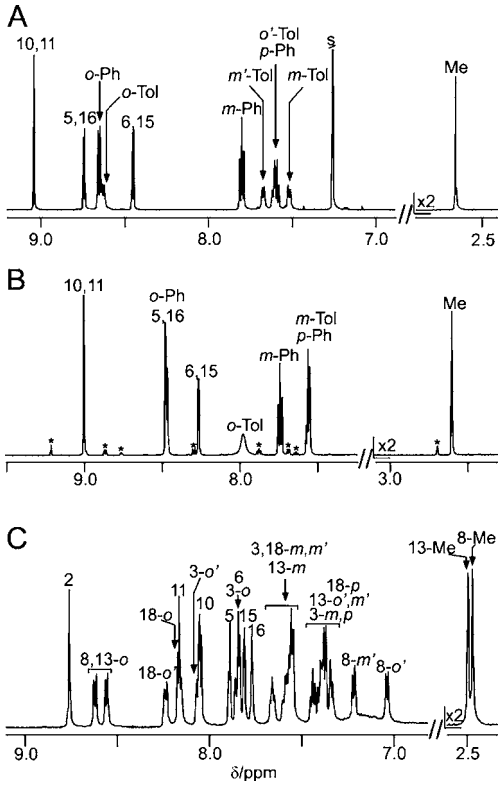

Figure 6. ^{1}H NMR spectra: (A) 7-Pd ($CDCl_3$, 282 K); (B) 7-Ni ($CDCl_3$, 300 K); (C) **14**-Pd (180 K, CD_2Cl_2). The residual resonances of **7** are marked with asterisks.

of the slower rotation rate. The fast rotation of all *meso*-aryls has been detected for 7-Ni at 300 K.

Reaction with Borohydride. 7-Pd reacts with sodium borohydride to produce aromatic palladium(II) thiaetheneporphyrin (Scheme 7).

Scheme 7. Formation of 14-Pd

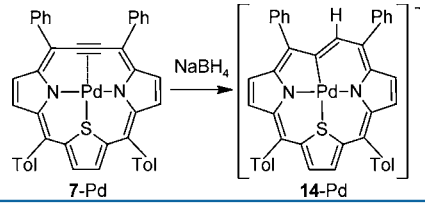

7-Pd **14**-Pd

The progress of transformation from 7-Pd to **14**-Pd has been directly followed by ^{1}H NMR (Figure 6, trace C) in conditions that afforded the best spectroscopic insight (i.e., 300 K, in dichloromethane-d_2 adding $NaBH_4$ in ethanol). Any attempt to isolate **14**-Pd failed. The ^{1}H NMR spectrum of **14**-Pd reflects symmetry lowering in comparison to 7-Pd. Two pyrrolic and one thiophene AB patterns and the unique H2 resonance can be easily identified. The C2 carbon atom of **14**-Pd produces a resonance at 122 ppm, which is consistent with its trigonal geometry. Thus, the Pd^{II}–η^2-C1C2 interaction has been replaced by the typical Pd^{II}–C σ bond (Pd–C1), affording the complex of a regular carbaporphyrinoid. Thus, the reaction with $NaBH_4$ can be considered as a specific case of 7-M reactivity. The deuterated derivative where a deuterium atom is bound to C2 has been synthesized as described above by replacing $NaBH_4$ in ethanol with $NaBD_4$ in methanol-d_4. The deuteration has resulted in the removal of the singlet at 8.76 ppm unambiguously assigned to the H2 position. The formation of **14**-Pd from 7-Pd can be described as the stereoselective *anti*-addition of palladium(II) and a hydride anion across the C1–C2 multiple bond. Formally, at the free base level, this transformation can be treated as an *anti*-addition of dihydrogen to thiaethyneporphyrin, yielding still aromatic 20-thiaetheneporphyrin **14** (Chart 6).

Chart 6

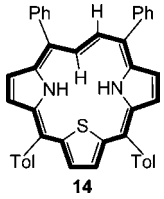

14

Initially, the analogous reactivity of 7-Ni toward $NaBH_4$ such as that determined for 7-Pd has been expected. The appropriate experiments followed by NMR led to the conclusion that demetalation might take place.

Formation of High-Spin Nickel(II) Species. Titration of 7-Ni with pyridine converted the low-spin species into the high-spin complex 7-Ni-py due to axial coordination (Scheme 8).

Scheme 8. Coordination of Pyridine to 7-Ni

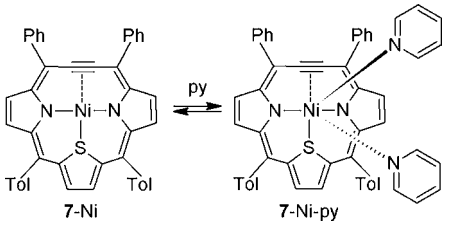

7-Ni **7**-Ni-py

The paramagnetic nickel(II) complex is readily identified by ^{1}H NMR (Figure 7). The spectrum resembles closely the pattern

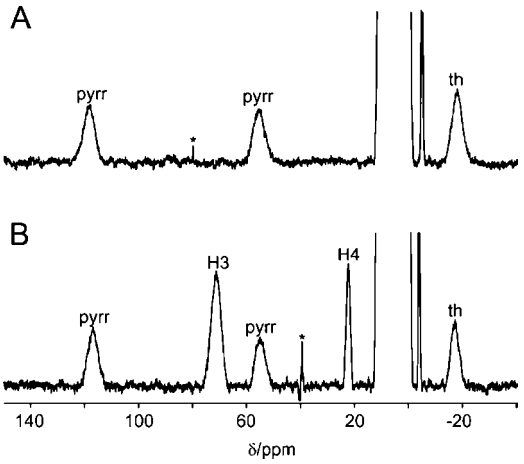

Figure 7. ^{1}H NMR spectrum of 7-Ni after the addition of (A) 0.25 equiv of pyridine-d_5 and (B) 0.25 equiv of pyridine (600 MHz, 200 K, CD_2Cl_2). Resonance assignments: pyrr, pyrrole; th, thiophene; H3, H4, protons of coordinated pyridine.

characteristic for paramagnetic nickel(II) thiaporphyrin with the upfield shift of the thiophene resonance and a large difference in contact shifts of downfield pyrrole resonances for β-H located in the same pyrrole ring.[57,60–62]

dx.doi.org/10.1021/ic2027175 | *Inorg. Chem.* 2012, 51, 3247–3260

The axial coordination of pyridine has been clearly confirmed by the detection of H3 and H4 resonances assigned readily by comparison of the NMR spectra collected for 7-Ni-py and 7-Ni-py-d_5. Two resonances of the two axially coordinated pyridines, located in the positions determined above, resemble those reported for pyridine coordinated to high-spin nickel(II) 21-thiaporphyrin.[61,62] In fact, the coordination equilibria of pyridine by nickel(II) thiaethyneporphyrin are quite complex. The selected and simplest example allows one to make quite a fundamental point. Namely, thiaethyneporphyrin is capable of accommodating both low- and high-spin nickel(II) cations, adjusting appropriately the size of a coordination crevice. The created coordination center provides a suitable environment, allowing stabilization of the organonickel(II) complex and revealing an unprecedented η^2-CC coordination of high-spin nickel(II).[10,63−67]

Molecular Structures of 7-Pd and 7-Ni. The geometry of 7-Pd as determined by X-ray crystallography (Figure 8) reflects

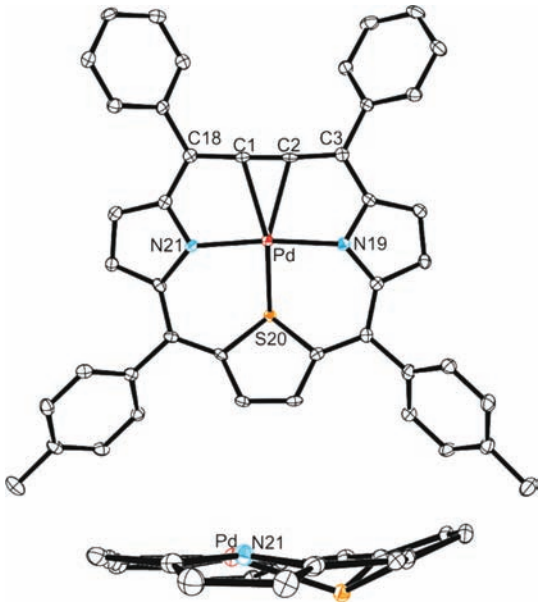

Figure 8. Molecular structure of 7-Pd (top, perspective view; bottom, side view with aryl groups omitted for clarity). The thermal ellipsoids represent 50% probability. Selected bond distances: Pd−N19, 2.029(2) Å; Pd−N21, 2.026(2) Å; Pd−S20, 2.177(1) Å; Pd−C1, 2.289(3) Å; Pd−C2, 2.315(3) Å. The bond lengths in the $C_{sp^2}C_{sp}C_{sp}C_{sp^2}$ (C18−C1−C2-C3) unit are 1.386(4), 1.257(4), and 1.388(4) Å. The bottom view presents the geometry of the side-on interaction between palladium(II) and thiophene.

the balance among constraints of the macrocycle ligand, the size of the palladium(II) ion, and the predisposition of the palladium(II) ion for square-planar geometry, resembling eventually the structure of palladium(II) vacataporphyrin, palladium(II) *p*-benziporphyrin,[33,57,60,62] and palladium 21-thiaporphyrin.[68,69]

The most notable feature of 7-Pd is the nature of the Pd···C1, Pd···C2, and Pd−S20 interactions. The bond-length pattern of aromatic 7 is preserved in 7-Pd. In particular, the acetylene unit approaches palladium(II) at distances much shorter [Pd···C1, 2.289(3) Å; Pd···C2, 2.315(3) Å] than the expected van der Waals contact (Pd···C, 3.3 Å)[70] but in the 2.110(7)−2.479(6) Å range limits of the typical values for palladium(II)-η^2-alkene complexes.[71−81] The relevant palladium(II)−η^2-CC bond distances for palladium(II)-η^2-alkyne vary in the 2.245(14)−2.487(15) Å range.[82,83] Thus, the palladium(II) ion interacts with thiaethyneporphyrin in an η^2-fashion engaging the C1 and C2 carbon atoms. For comparison, the palladium(0) complexes containing alkenes and/or alkynes built in the macrocyclic structure afforded the formation of palladium(0)−η^2-alkene [2.185(3)−2.197(4) Å] or palladium(0)−η^2-alkyne [2.107(4)−2.140(6) Å] bonds.[84] A weak interaction has been observed for palladium(II) *p*-benziporphyrin and palladium(II) naphthiporphyrin complexes both in solution and in the solid state; albeit, in these cases, the CC fragment built-in arene units are involved.[48,69]

The C18−C1−C2−C3 butyne moiety is slightly bent toward palladium(II), as is clearly reflected by the appropriate bond angles [C18−C1−C2, 175.7(3)°; C1−C2−C3, 178.5(3)°]. While the thiophene ring is planar, it is sharply bent out of the plane of the porphyrin. The shape of the porphyrin resembles that seen in metal(II) complexes of 21-thiaporphyrins.[63] The dihedral angle between the thiophene plane and the Pd−N19−N21−C1−C2 plane is 24.2°. This bending opens up the center of the porphyrin to accommodate palladium(II) and allows palladium(II) to interact with the thiophene sulfur in a side-on fashion. The angle between the center of thiophene and the Pd−S20 bond is 132.5°. Similar angles are found in palladium 21-thiaporphyrin.[68] The Pd−S20 distance, 2.177(1) Å, is clearly a bonding distance. Thus, the thiophene is σ-bonded to palladium through sulfur, which has pyramidal geometry.

7-Ni reveals structural features similar to those of 7-Pd (Figure 9). Some differences result from constraints imposed by smaller

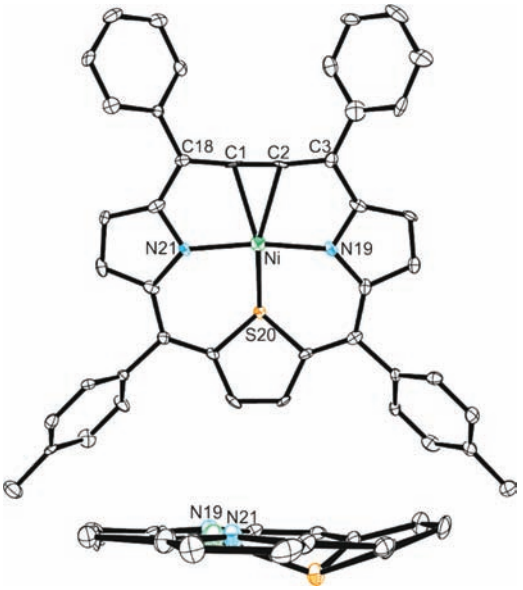

Figure 9. Molecular structure of 7-Ni (top, perspective view; bottom, side view with aryl groups omitted for clarity). The thermal ellipsoids represent 50% probability. Selected bond distances: Ni−N19, 1.964(4) Å; Ni−N21, 1.956(4) Å; Ni−S20, 2.087(1) Å; Ni−C1, 2.213(5) Å; Ni−C2, 2.229(5) Å. The bond lengths in the $C_{sp^2}C_{sp}C_{sp}C_{sp^2}$ (C18−C1−C2−C3) unit are 1.345(6), 1.238(5), and 1.362(6) Å. The bottom view presents the geometry of the interaction between nickel(II) and thiophene.

cationic radii of low-spin nickel(II), which are expected and clearly demonstrated by shorter Ni−N and Ni−S bond distances. Thus, the nickel(II) ion interacts with thiaethyneporphyrin in a η^2-fashion, engaging the C1 and C2 carbon atoms. The C18−C1−C2−C3 butyne moiety of 7-Ni is bent toward nickel(II) stronger than for 7-Pd, as is clearly reflected by the appropriate

dx.doi.org/10.1021/ic2027175 | Inorg. Chem. 2012, 51, 3247−3260

bond angles [C18−C1−C2, 173.5(7)°; C1−C2−C3, 174.5(7)°]. The C1C2 unit approaches nickel(II) at distances much shorter [Ni···C1, 2.213(5) Å; Ni···C2, 2.229(5) Å] than the expected van der Waals contact (Ni···C, 3.4 Å)[70] but in the upper limit of nickel(II)−η^2-alkene bond lengths, which vary in the wide range 1.950(3)−2.285(7) Å.[85−89] For comparison, the representative nickel(0)−η^2-CC bond distances are also given: nickel(0)−η^2-alkene [2.024(6) Å],[90] nickel(0)−η^2-benzene [2.021(1) Å],[91] nickel(0)−η^2-allene [1.916(5) Å],[92] and nickel(0)−η^2-alkyne [1.875(4) Å].[93,94] The relevant weak interaction has been observed for the high-spin nickel(II) *p*-benziporphyrin complex both in solution and in the solid state [Ni···C, 2.583(4) Å].[47] In fact, paramagnetic organonickel compounds are extremely rare.[10,63,64] The few examples include species with a σ-bound methyl group [Ni(I)−C distance of 2.04(1) Å][65,66] or a η^5-cyclopentadienyl group (mean distance of 2.27 Å),[66] and the iodonickel(II) complex of 2,21-dimethylated N-confused porphyrin [2.404(9) Å].[67]

The dihedral angle between the thiophene plane and the Ni−N19−N21−C1−C2 plane is 20.1°. Nickel(II) interacts with the thiophene sulfur in a side-on fashion. The angle between the center of the thiophene and the Ni−S20 bond is 136°. Similar angles are found in the nickel(II) 21-thiaporphyrins.[95,96]

Density Functional Theory (DFT) Studies: Ethyneporphyrins. The magnetic manifestations of aromaticity and antiaromaticity of **7** and its two-electron-oxidized derivative can easily be observed using ^{1}H NMR spectroscopy. However, this method does not provide detailed information on the structural consequences of electron delocalization in these two species. Furthermore, in the absence of X-ray structural data, it is difficult to ascertain whether [**13**-H$_2$]$^{2+}$ does exhibit bond alternation along the [16]annulene pathway, expected for a 4*n* π-electron system. To address these issues, we carried out DFT calculations of **7** and [**13**-H$_2$]$^{2+}$, performing full geometry optimizations at the B3LYP/6-31G** level. A genuine energy minimum was obtained for **7** and [**13**-H$_2$]$^{2+}$.

The DFT-optimized geometry of **7** closely resembles that determined by X-ray crystallography, revealing an equalization of the C−C bond along the π delocalization route (Figure 10). The DFT structure of [**13**-H$_2$]$^{2+}$ shows bond localization, as expected of an antiaromatic planar [4*n*]annulenoid system. In fact, the known structures of 16 π-electron porphyrin rings demonstrated the presence of bond alternation characteristic of antiaromatic structures in contrast to aromatic 18 π-electron porphyrins.[97−102] To address the issue of macrocyclic conjugation on the built-in acetylenic moiety, Wiberg bond indices have been applied to estimate bond orders of C18−C1, C1−C2, and C2−C3 bonds in thiaethyneporphyrin **7** and related compounds ([**13**-H$_2$]$^{2+}$, 7-Pd, 7-Ni; Table 1).[103] In comparison to **11**, applied here as a suitable acetylene-like reference, the indices of C1−C2 in **7**, [**13**-H$_2$]$^{2+}$, 7-Pd, and 7-Ni approach values that are expected for the double bond. At the same time, the indices for C18−C1 and C2−C3 bonds approach the limit for the aromatic bond. Thus, Wiberg bond indices reflect the essential role of cumulene contributor **7**-2 in the description of 20-thiaethyneporphyrin.

Nucleus-independent chemical shifts (NICS) have been proposed by Schleyer et al. as a computational measure of aromaticity that is related to experimental magnetic criteria.[104,105] A NICS is defined as the negative shielding value computed at the center of a ring. The NICS method has been used to assess the aromaticity of annulenes or porphyrins[106,107] and their analogues.[108−111] NICS values were calculated for **7** and [**13**-H$_2$]$^{2+}$ using the GIAO method at the optimization level for the central 15-membered ring. A comparison of the center ring NICS (calculated for B3LYP/6-31G** geometries) values shows that they are good indicators of macrocyclic aromaticity. For the Hückel aromatic system **7**, the central NICS value is negative (−13.05 ppm) and comparable with that reported for a porphyrin (−16.5 ppm).[106] For the antiaromatic structure of [**13**-H$_2$]$^{2+}$, the

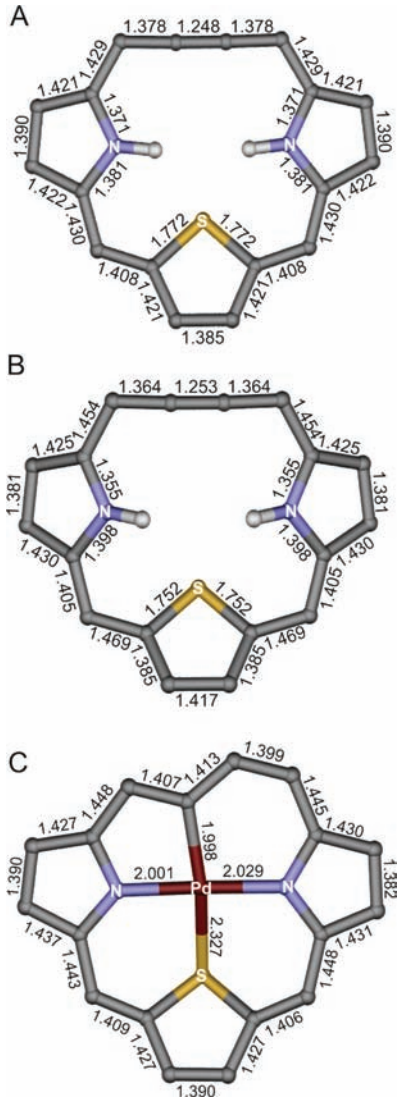

Figure 10. Calculated geometries and bond lengths (in Å) of structures **7** (A), [**13**-H$_2$]$^{2+}$ (B), and **14**-Pd (C). Nitrogen and sulfur are shown in blue and yellow, respectively. Outer hydrogen atoms and meso substituents are omitted for clarity. **7** and [**13**-H$_2$]$^{2+}$ have effective C_s symmetry, and the equivalent bond distances are equal within the given accuracy.

Table 1. Wiberg Bond Indices

	bond		
compound	C18−C1	C1−C2	C2−C3
11	1.011[a]	2.8475[b]	1.011[c]
7	1.4475	2.2621	1.4475
[**13**-H$_2$]$^{2+}$	1.5692	2.1467	1.5792
7-Pd	1.4201	2.0097	1.4201
7-Ni	1.3681	2.1604	1.3681

[a]C1−C2. [b]C2−C3. [c]C3−C4.

dx.doi.org/10.1021/ic2027175 | *Inorg. Chem.* 2012, 51, 3247−3260

center ring NICS is positive (+18.95 ppm). This value is larger than the NICS obtained for [20]annulene (+12.1 ppm).[112]

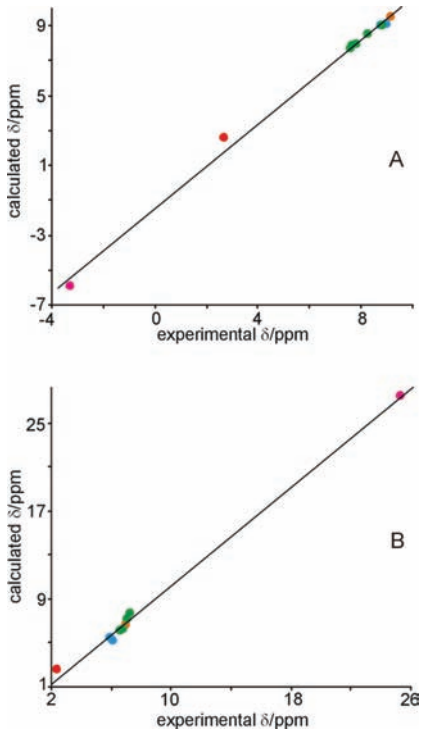

Figure 11. Linear correlation between calculated and experimental values of chemical shifts for (A) **7** and (B) $[\mathbf{13}\text{-}H_2]^{2+}$ (orange, thiophene; blue, pyrrole; pink, NH; green, aryl; red, methyl).

^{1}H NMR chemical shifts have been calculated using the GIAO–B3LYP method for the optimized (at the B3LYP/6-31G** level) geometries of aromatic **7** and antiaromatic $[\mathbf{13}\text{-}H_2]^{2+}$ (Figure 11). In the described cases, we have been in a unique position to compare the experimental and calculated chemical shifts assigned to aromatic and antiaromatic structures confined in the frame of ethyneporphyrin geometries. We have concluded that there is a satisfactory qualitative agreement for each considered set of theoretical and experimental data readily demonstrated by linear correlations between the calculated and experimental chemical shifts (Figure 11).

DFT Calculations: Metalloporphyrinoids. The principal geometries of **7**-Ni, **7**-Pd, and **14**-Pd were subjected to a DFT optimization at the B3LYP level of theory with the LANL2D basis set for palladium complexes and the 6-31G** basis set for nickel complexes. The final geometries are shown in Figure 12 and S9 in the Supporting Information. In each case, a genuine energy minimum was obtained. Significantly, the DFT-optimized structural parameters of **7**-Pd and **7**-Ni are essentially similar to those determined by X-ray crystallography, which adds credibility to the geometry of the DFT-optimized structure of **14**-Pd. ^{1}H NMR chemical shifts have been calculated using the GIAO–B3LYP method for the optimized geometries of **7**-Pd, **7**-Ni, and **14**-Pd. Linear correlations between the calculated and experimental values of the chemical shifts for each complex have been determined (Figures S10–S12 in the Supporting Information).

The interaction involving metal(II) and the ethyne fragment in **7**-M is of special interest. A comparison of the properties of Wiberg bond indices is helpful in discussing the

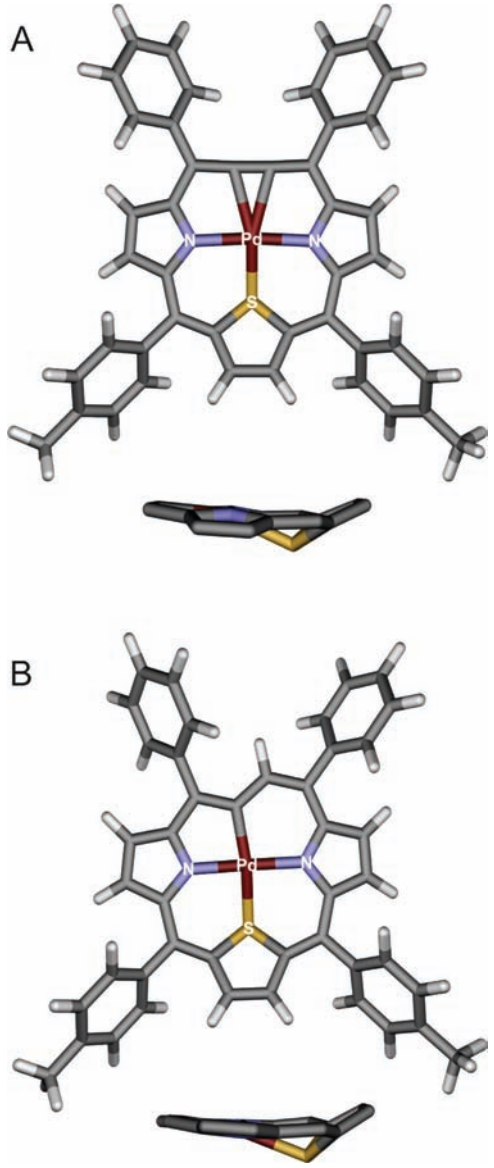

Figure 12. Geometries of **7**-Pd (A) and **14**-Pd (B) obtained in a DFT study. Projections emphasize the conformations of the macrocycles. Outer hydrogen atoms and meso substituents (bottom views) are omitted for clarity.

palladium(II)···η^2-C1C2 and nickel(II)···η^2-C1C2 interaction in **7**-Pd and **7**-Ni. The data gathered in Table 2 provide examples

Table 2. Wiberg Bond Indices

	compound	
bond	**7**-Pd	**7**-Ni
M–C1	0.1649	0.1589
M–C2	0.1650	0.1589
M–N19	0.4700	0.3888
M–N21	0.4700	0.3888
M–S20	0.6329	0.5514

of the typical coordination bonds M–N and M–S and the metal(II)···η^2-C1C2 itself. Evidently, the metal(II)···C1 and metal(II)···C2 interactions have significant bonding character, albeit smaller than simultaneously coordinating nitrogen atoms.

dx.doi.org/10.1021/ic2027175 | *Inorg. Chem.* 2012, 51, 3247–3260

CONCLUSION

Thiaethyneporphyrin is an aromatic porphyrinoid that presents the essential features of [18]triphyrin(4.1.1). The combination of two structural motifs of 21-thiaporphyrin and ethyne in thiaethyneporphyrin provided a unique opportunity to study metal(II)···η^2-C1C2 interactions. In this contribution, we have demonstrated that 20-thiaethyneporphyrin acts as a macrocyclic ligand to palladium(II) or nickel(II), which are suitably held *via* two pyrrolic nitrogen and one thiophenic sulfur atoms in the T-like fashion, being conveniently exposed to interaction with a conjugated four-carbon linker of porphyrinoid. Eventually, two fundamental patterns of interactions between metal(II) and a four-carbon conjugated moiety have been recognized. The first one corresponds to a regular η^2-type bond and involves the C1C2 fragment. Significantly, the CC unit is located in the plane defined by the remaining three donor atoms. The second mode was revealed once palladium(II) thiaethyneporphyrin reacted with sodium borohydride, yielding palladium(II) thiaetheneporphyrin. The profound structural changes due to the addition of hydride and palladium(II) to the C1C2 unit allowed one to create the regular Pd−C σ bond, demonstrating that [18]thiatriphyrins(4.1.1) can act as "true" carbaporphyrinoids. It is significant to emphasize that the coordination core of [18]thiatriphyrins(4.1.1) is quite flexible, accommodating peculiar organometallic compounds represented in this work by high-spin nickel(II) organometallic species. In terms of the characterization of intermediates involved in selective C−C bond activation by metals under mild conditions, the reported organometallic compounds provide suitable structural models of the transient species. Previously reported [18]triphyrins(6.1.1) (vacataporphyrin) applied as a ligand toward metal(II) demonstrated the peculiar plasticity of its molecular and electronic structure.[33,34,64,113,114] The present contribution revealed that the length of the meso bridge allows one to control the electronic structure and coordination properties of this class of porphyrinoids. Generally, [*N*]triphyrins(*n*.1.1) provide a stimulating environment to explore the specific issues of organometallic chemistry, applying the macrocyclic platform concept as the suitable approach.

EXPERIMENTAL SECTION

Materials. 2,5-Bis(*p*-tolylhydroxymethyl)thiophene was prepared *via* a previously reported procedure by Ulman and Manassen.[115] Solvents like methanol, ethanol, and *n*-hexane, at least pure grade, were used without purification. Tetrahydrofuran (THF), toluene and N,N-dimethylformamide (DMF) were purified *via* pushing through absorber column (M Braun SPS-800 system). Dichloromethane and triethylamine were distilled over CaH_2. Dichloromethane-d_2 was used as received. Chloroform-*d* was prepared directly before use by passing through a basic alumina column. Inorganic salts were used without purification.

1,4-Diphenyl-2-butyne-1,4-diol (8) was prepared *via* a modified procedure reported by Krupowicz and Sapiecha.[36,37] THF (200 mL), ethylmagnesium bromide (40 mL, 1 M in THF, 0.04 mol), and ethynylmagnesium bromide (80 mL, 0.5 M in THF, 0.04 mol) were placed in a 500-mL round-bottomed flask. The mixture was stirred under a nitrogen atmosphere for 16−18 h. Then the reaction mixture was heated until reflux, and a solution of benzaldehyde (0.08 mol) in THF (20 mL) was added dropwise over a period of 20 min, after which reflux was maintained for 7 h. The mixture was cooled to room temperature and stirred overnight. The reaction mixture was quenched with water (100 mL) and extracted with diethyl eter (3 × 50 mL). The combined organic phases were dried (anhydrous $MgSO_4$) and evaporated to dryness on a rotary evaporator to give a yellow-brown oil. Recrystallization from dichloromethane/*n*-hexane produced **8** with 47% yield (white crystals, 4.43 g). ^{1}H NMR (600 MHz, CD_2Cl_2, 300 K): δ 7.54 (4H, *o*-Ph), 7.39 (4H, *m*-Ph), 7.34 (2H, *p*-Ph), 5.55 (2H, H1, H4), 2.43 (2H, OH). ^{13}C NMR (150.90 MHz, CD_2Cl_2, 300 K): δ 142.2, 130.2, 130.0, 128.1, 87.9, 66.0. HR-MS (ESI, *m*/*z*): 221.0992 (221.0966 calcd for $[C_{16}H_{14}O_2 - OH]^+$).

Dicobalt Complex of 1,4-Diphenyl-2-butyne-1,4-diol (9). Dicobalt octacarbonyl (4.31 g, 12.6 mmol) was added to a solution of **8** (3.0 g, 12.6 mmol) in THF (150 mL). The mixture was stirred in a nitrogen atmosphere for 24 h. Then the solvent was evaporated to dryness, and the residue was purified by chromatography on silica gel. The main red fraction eluted with dichloromethane was collected to give **9** with 95% yield (6.61 g). ^{1}H NMR (500 MHz, $CDCl_3$, 298 K): two stereoisomers were observed, δ 7.5−7.3 (1,4-*o*, *m*, *p*), 5.96 (H1, H4), 5.80 (H1, H4), 3.40 (OH), 3.30 (OH). ^{13}C NMR (125.7 MHz, $CDCl_3$, 300 K): δ 198.4, 143.6, 143.2, 128.7, 128.5, 128.3, 128.2, 125.7, 125.6, 75.1, 74.6.

Dicobalt Complex of 1,4-Diphenyl-1,4-di(pyrrol-2-yl)but-2-yne (10). Compound **9** (1.64 g, 3.14 mmol) was dissolved in dry pyrrole (8.69 mL), and the solution was purged with nitrogen gas for 10 min. Then trifluoroacetic acid (TFA; 1.2 mL, 15.7 mmol) was added, and the mixture was stirred in a nitrogen atmosphere for 2 h. Next 50 mL of freshly distilled dichloromethane was added, and the solution was neutralized by the addition of a 40% solution of sodium hydroxide (30 mL). The organic layer was washed with water (3 × 40 mL) and dried (anhydrous $MgSO_4$), and the solvent was evaporated to dryness. The residue was purified by chromatography on silica gel. The main brown-red fraction eluted with a dichloromethane/hexane fraction (1:2, v/v) was collected to give **10** with 60% yield (brown-red oil, 1.17 g). ^{1}H NMR (500 MHz, $CDCl_3$, 298 K): two stereoisomers were observed, δ 7.85, 7.74, 7.43−7.29, 6.60, 6.57, 6.14, 6.12, 5.37, 5.34. ^{13}C NMR ($CDCl_3$, 298 K): δ 198.8, 142.7, 142.6, 132.3, 132.0, 128.9, 128.8, 128.4, 127.7, 127.6, 118.2, 117.6, 108.4, 108.3, 107.7, 107.5, 103.0, 102.7, 49.8, 49.3.

1,4-Diphenyl-1,4-di(pyrrol-2-yl)but-2-yne (11). Compound **10** (0.2 g, 0.32 mmol) was dissolved in ethanol (6.7 mL); then $Fe(NO_3)_3{\cdot}9H_2O$ (0.52 g, 1.28 mmol) was added, and the mixture was stirred for 20 min. Subsequently, the mixture was combined with water (15 mL) and extracted with diethyl ether (3 × 20 mL). The organic layer was dried (anhydrous $MgSO_4$), and the solvent was evaporated to dryness. The residue was purified by chromatography on silica gel. A second yellow fraction eluted with dichloromethane/*n*-hexane (1:1, v/v) was collected to give **11** with 30% yield (yellow oil, 32 mg). ^{1}H NMR (600 MHz, CD_2Cl_2, 300 K): δ 8.16 (2H, NH), 7.43 (4H, *o*-Ph), 7.36 (4H, *m*-Ph), 7.29 (2H, *p*-Ph), 6.67 (2H, pyr), 6.11 (2H, pyr), 6.02 (2H, pyr), 5.20 (2H, H1, H4). ^{13}C NMR (150.90 MHz, CD_2Cl_2, 300 K): δ 142.2 (*i*-Ph), 132.4 (α-pyr), 130.3 (*m*-Ph), 129.1 (*o*-Ph), 128.8 (*p*-Ph), 118.9 (pyr), 110.1 (pyr), 107.8 (pyr), 84.9 (C2, C3), 38.4 (C1, C4). HR-MS (ESI, *m*/*z*): 337.1755 (337.1705 calcd for $[C_{24}H_{20}N_2 + H]^+$).

3,18-Diphenyl-8,13-di-*p*-tolyl-20-thiaethyneporphyrin (7). Compound **11** (314 mg, 0.935 mmol) and 2,5-bis-(tolylhydroxymethyl)thiophene (303 mg, 0.935 mmol) were dissolved in freshly distilled dichloromethane (312 mL) in a 500-mL round-bottomed flask equipped with stirring bar and a nitrogen inlet. Nitrogen was bubbled through the solution for 15 min; then boron trifluoride−diethyl ether (117 μL, 0.935 mmol) was added, and the mixture was stirred in the dark for 15 min under a nitrogen atmosphere. Triethylamine (130 μL, 0.935 mmol) and 2,3-dichloro-5,6-dicyano-*p*-benzoquinone (DDQ; 424 mg, 1.87 mmol) were added, and the solution was stirred for a further 30 min. Then the solvent was evaporated to dryness, and the residue was purified by chromatography on basic allumine (II°). The main orange fraction eluted with dichloromethane was collected and recrystallized from dichloromethane/methanol to give **7** with 33% yield (191 mg). UV−vis [λ_{max}, nm (log ε, M^{-1} cm^{-1})]: 439 (5.1), 508 (4.2), 539 (3.9), 630 (3.3), 710 (3.1). HR-MS (ESI, *m*/*z*): 620.2290 (620.2286 calcd for $[C_{44}H_{32}N_2S]^{\bullet+}$). ^{1}H NMR (600 MHz, $CDCl_3$, 300 K): δ 9.16 (s, 2H, H10, H11), 8.97 (dd, ^3J = 4.4 Hz, ^4J = 2.2 Hz, 2H, H5, H16), 8.84 (d, ^3J = 7.6 Hz, 4H, 3,18-*o*), 8.75 (dd, ^3J = 4.4 Hz, ^4J = 2.2 Hz, 2H, H6, H15), 8.27 (d, ^3J = 7.8 Hz, 4H, 8,13-*o*), 7.84 (t, ^3J = 7.6 Hz, 4H,

dx.doi.org/10.1021/ic2027175 | *Inorg. Chem.* 2012, 51, 3247−3260

3,18-*m*), 7.65 (d, ^3J = 7.8 Hz, 4H, 8,13-*m*), 7.60 (t, ^3J = 7.3 Hz, 2H, 3,18-*p*), 2.68 (s, 6H, CH_3), −3.29 (bs, 2H, H19, H21). ^{13}C NMR (150.90 MHz, $CDCl_3$, 300 K): δ 140.4 (3,18-*ipso*), 137.7 (8,13-*p*), 137.5 (8,13-*ipso*), 136.2 (9,12), 134.3 (8,13-*o*), 133.9 (7,14), 132.7 (3,18-*o*), 132.3 (4,17), 129.5 (10,11), 129.2 (3,8,13,18-*m*), 126.9 (3,18-*p*), 122.6 (6,15), 117.9 (1,2), 117.5 (5,16), 116.8 (8,13), 102.3 (3,18), 21.5 (Me).

Dehydro-3,18-diphenyl-8,13-di-*p*-tolyl-20-thiaethyneporphyrin Dication ([13-H_2^{2+}]). The solution of **7** in $CDCl_3$ or CD_2Cl_2 was placed in an NMR tube (typically, a sample of ∼1−2 mg of **16**). Then excess of DDQ in the presence of HBF_4 etherate was added, and a change of color from orange to brown-red was observed. The oxidation of **7** afforded a ^{1}H NMR spectrum readily assigned to [**13**-H_2]$^{2+}$. HR-MS (ESI, *m*/*z*): 619.2206 (619.2208 calcd for [$C_{44}H_{30}N_2S$ + H]$^+$). ^{1}H NMR (600 MHz, $CDCl_3$, 300 K): δ 25.35 (s, 2H, H19, H21), 7.25 (t, ^3J = 7.5 Hz, 2H, 3,18-*p*), 7.10 (t, ^3J = 7.9 Hz, 4H, 3,18-*m*), 7.06 (d, ^3J = 8.1 Hz, 4H, 8,13-*m*), 6.96 (s, 2H, H10, H11), 6.80 (d, ^3J = 8.3 Hz, 4H, 8,13-*o*), 6.60 (d, ^3J = 7.9 Hz, 4H, 3,18-*o*), 6.08 (dd, ^3J = 5.0 Hz, ^4J = 1.9 Hz, 2H, H5, H16), 5.96 (dd, ^3J = 5.0 Hz, ^4J = 1.9 Hz, 2H, H6, H15), 2.34 (s, 6H, Me).

***iso*-Thiaethyneporphyrin (12′-H$^+$).** The solution of **7** in CD_2Cl_2 was placed in an NMR tube (typically, a sample of ∼1−2 mg of **7**). The titration of **7** was carried out with HBF_4 etherate or TFA at 298 K. The progress of the reaction was followed by NMR spectroscopy. ^{1}H NMR (600 MHz, CD_2Cl_2, 300 K): δ 9.65, 9.50, 8.06, 7.81, 7.70, 7.59−7.55, 7.54, 7.52, 7.46, 7.44, 7.32, 7.27, 7.24, 7.23, 7.12, 6.35, 5.50, 2.52, 2.39.

Nickel(II) Complex of 3,18-Diphenyl-8,13-di-*p*-tolyl-20-thiaethyneporphyrin (7-Ni). Nickel(II) acetate (28 mg, 0.1 mmol) in 5 mL of DMF was added to a dark-orange toluene solution of **7** (7 mg, 0.01 mmol). The mixture was refluxed under nitrogen. The progress of the reaction was followed by UV−vis spectroscopy. After the disappearance of absorption peaks ascribed to the starting material (it usually takes ∼5 h), the solvent was evaporated to dryness and the residue was purified by chromatography on silica gel. The main brown-red fraction eluted with dichloromethane was collected and recrystallized from dichloromethane/*n*-hexane to give 7-Ni with 50% yield. UV−vis [λ_{max}, nm (log ε, M^{-1} cm^{-1})]: 291.0 (4.4), 435.0 (4.6), 595.0 (3.7). HR-MS (ESI, *m*/*z*): 676.1483 (676.1483 calcd for [$C_{44}H_{30}N_2SNi$]$^{\bullet+}$). ^{1}H NMR (500 MHz, CD_2Cl_2, 300 K): δ 8.97 (s, 2H, H10, H11), 8.44 (d, ^3J = 4.5 Hz, 2H, H5, H16), 8.43 (d, ^3J = 7.6 Hz, 4H, 3,18-*o*), 8.22 (d, ^3J = 4.5 Hz, 2H, H6, H15), 7.94 (bs, 4H, 8,13-*o*), 7.72 (t, ^3J = 7.6 Hz, 4H, 3,18-*m*), 7.55 (t, ^3J = 7.6 Hz, 2H, 3,18-*p*), 7.54 (d, ^3J = 8.0 Hz, 4H, 8,13-*m*), 2.59 (s, 6H, Me). ^{13}C NMR (150.90 MHz, CD_2Cl_2, 300 K): δ 160.9 (α-pyr), 145.9 (α-pyr), 140.0 (8,13-*p*), 139.5 (8,13-*ipso*), 138.7 (3,18-*ipso*), 133.9 (8,13-*o*), 132.6 (3,18-*o*), 130.8 (3,18-*m*), 130.7 (8,13-*m*), 129.7 (10,11), 128.9 (3,18-*p*), 127.1 (9,12), 127.0 (6,15), 124.2 (8,13), 124.0 (5,16), 116.8 (1,2), 105.9 (3,18), 22.8 (Me).

Dipyridinenickel(II) Complex of 3,18-Diphenyl-8,13-di-*p*-tolyl-20-thiaethyneporphyrin (7-Ni-py). The solution of 7-Ni in CD_2Cl_2 was placed in an NMR tube (typically, a sample of ∼1−2 mg of 7-Ni). Titration of 7-Ni with pyridine at 200 K afforded the ^{1}H NMR spectrum readily assigned to 7-Ni-py. ^{1}H NMR (600 MHz, CD_2Cl_2, 200 K): δ 117.0 (pyrr), 71.2 (H3), 54.9 (pyrr), 22.3 (H4), −17.4 (th).

Palladium(II) Complex of 3,18-Diphenyl-8,13-di-*p*-tolyl-20-thiaethyneporphyrin (7-Pd). Palladium(II) acetate (36 mg, 0.16 mmol) was added to a dark-orange toluene solution of **7** (10 mg, 0.016 mmol). The mixture was refluxed. The progress of the reaction was followed by UV−vis spectroscopy. After the disappearance of absorption peaks ascribed to the starting material (it usually takes ∼4 h), the solvent was evaporated to dryness and the residue was purified by chromatography on silica gel. The main brown-red fraction eluted with dichloromethane was collected and recrystallized from CH_2Cl_2/CH_3OH to give 7-Pd with 60% yield. UV−vis [λ_{max}, nm (log ε, M^{-1} cm^{-1})]: 285.5 (4.4), 373.0 (4.1), 462.0 (4.9), 578.5 (3.8). HR-MS (ESI, *m*/*z*): 724.1175 (724.1180 calcd for [$C_{44}H_{30}N_2S^{106}Pd$]$^{\bullet+}$). ^{1}H NMR (600 MHz, CD_2Cl_2, 300 K): δ 9.04 (s, 2H, H10, H11), 8.72 (d, ^3J = 4.5 Hz, 2H, H5, H16), 8.64 (d, ^3J = 7.6 Hz, 4H, 3,18-*o*), 8.61 (bs, 2H, 8,13-*o*), 8.41 (d, ^3J = 4.5 Hz, H6, H15), 7.81 (t, ^3J = 7.6 Hz, 4H, 3,18-*m*), 7.69 (bs, 2H, 8,13-*o*), 7.60 (t, ^3J = 7.6 Hz, 2H, 3,18-*p*), 7.56 (bs, 2H, 8,13-*m*), 7.53 (bs, 2H, 8,13-*m*), 2.65 (s, 6H, Me). ^{1}H NMR (600 MHz, $CDCl_3$, 282 K): δ 9.04 (s, 2H, H10, H11), 8.74 (d, ^3J = 4.6 Hz, 2H, H5, H16), 8.64 (d, ^3J = 7.8 Hz, 4H, 3,18-*o*), 8.62 (d, ^3J = 7.7 Hz, 2H, 8,13-*o*), 8.44 (d, ^3J = 4.6 Hz, H6, H15), 7.79 (t, ^3J = 7.8 Hz, 4H, 3,18-*m*), 7.67 (d, ^3J = 7.5 Hz, 2H, 8,13-*m*′), 7.60 (d, 2H, 8,13-*o*′), 7.58 (t, ^3J = 7.4 Hz, 2H, 3,18-*p*), 7.51 (d, ^3J = 7.5 Hz, 2H, 8,13-*m*), 2.64 (s, 6H, Me). ^{13}C NMR (150.90 MHz, $CDCl_3$, 300 K): δ 159.5 (α-pyr), 143.1 (α-pyr), 140.0 (8,13-*p*), 139.7 (8,13-*ipso*), 139.4 (3,18-*ipso*), 136.6 (8,13-*o*), 133.4 (3,18-*o*), 131.0 (3,18-*m*), 130.9 (10,11), 130.7 (8,13-*m*), 129.0 (3,18-*p*), 128.0 (9,12), 125.7 (8,13), 124.5 (5,16), 124.2 (6,15), 115.8 (1,2), 107.2 (3,18), 22.8 (Me).

Palladium(II) Complex of 3,18-Diphenyl-8,13-di-*p*-tolyl-20-thiaetheneporphyrin (14-Pd). The solution of 7-Pd in CD_2Cl_2 was placed in an NMR tube (typically, a sample of ∼1−2 mg of 7-Pd). Then the ethanol solution of $NaBH_4$ was added gradually (at 30 min intervals) through a 25 μL microsyringe. The addition of a reducting agent was stopped when the entire amount of 7-Pd was converted to **14**-Pd. HR-MS (ESI, *m*/*z*): 725.1265 (725.1248 calcd for [$C_{44}H_{31}N_2S^{106}Pd$]$^-$). ^{1}H NMR (600 MHz, CD_2Cl_2, 180 K): δ 8.76 (s, 1H, H2), 8.62 (d, 1H, ^3J = 7.8 Hz, 8-*o*), 8.56 (d, ^3J = 7.8 Hz, 1H, 13-*o*), 8.24 (d, ^3J = 7.3 Hz, 1H, 18-*o*′), 8.17 (d, ^3J = 5.3 Hz, 1H, H11), 8.15 (d, ^3J = 7.3 Hz, 1H, 18-*o*), 8.06 (d, ^3J = 7.5 Hz, 1H, 3-*o*′), 8.05 (d, ^3J = 5.3 Hz, 1H, H10), 7.89 (d, ^3J = 3.8 Hz, 1H, H5), 7.85 (d, ^3J = 7.3 Hz, 3-*o*), 7.84 (d, ^3J = 3.8 Hz, 1H, H6), 7.81 (d, ^3J = 3.8 Hz, 1H, H15), 7.77 (d, ^3J = 3.6 Hz, 1H, H16), 7.66 (t, ^3J = 7.3 Hz, 1H, 18-*m*′), 7.59 (t, ^3J = 7.3 Hz, 1H, 18-*m*), 7.57 (t, ^3J = 7.1 Hz, 1H, 3-*m*′), 7.55 (d, 1H + 1H, 8,13-*m*), 7.44 (t, ^3J = 7.4 Hz, 1H, 3-*m*), 7.40 (t, ^3J = 7.4 Hz, 1H, 18-*p*), 7.39 (t, 1H, 3-*p*), 7.37 (d, ^3J = 7.8 Hz, 1H, 13-*o*′), 7.33 (d, ^3J = 7.8 Hz, 1H, 13-*m*′), 7.21 (d, ^3J = 7.8 Hz, 1H, 8-*m*′), 7.03 (d, ^3J = 7.8 Hz, 1H, 8-*o*′), 2.49 (s, 3H, 13-Me), 2.47 (s, 3H, 8-Me). ^{13}C NMR (150.90 MHz, $CDCl_3$, 300 K): δ 153.1, 150.8, 148.1, 140.7, 140.0, 139.7, 139.6, 137.4, 137.2, 137.1, 136.3, 135.8−135.7, 135.2, 134.3, 133.9, 133.7, 133.5, 132.7, 132.5, 132.1, 130.8, 130.6, 129.5, 129.3−129.2, 129.1, 129.0, 128.8, 128.4, 128.1, 127.7, 127.6, 127.1, 126.1−125.9, 122.1, 122.0 (C2), 119.2, 118.1, 115.9, 22.0.

Instrumentation. NMR spectra were measured on Bruker Avance 500 MHz and Bruker Avance 600 MHz spectrometers. ^{1}H and ^{13}C NMR shifts were referenced to the residual resonances of deuterated solvents. Two-dimensional NMR spectra were recorded typically with 2048 data points in the t2 domain and up to 1024 points in the t1 domain, with a 1 s recovery delay. Absorption spectra were recorded on a Varian Carry-50 Bio spectrophotometer. Mass spectra (high resolution and accurate mass) were recorded on a Brüker micro-TOF-Q spectrometer using the electrospray technique. X-ray-quality crystals of **7** and 7-Pd were prepared by the diffusion of methanol or *n*-hexane and *o*-dichlorobenzene, respectively, into a chloroform solution contained in a tube stored in a refrigerator. X-ray-quality crystals of 7-Ni and **11** were prepared by the diffusion of *n*-hexane or *n*-heptane, respectively, into a dichloromethane solution contained in a tube stored at room temperature. Data were collected at 100 K for **7** and 7-Pd, 7-Ni and at 110 K for **11** on an Xcalibur PX-k geometry diffractometer, with Mo Kα radiation (λ = 0.71073 Å). Data were corrected for Lorentz and polarization effects. An analytical absorption correction was applied for 7-Pd and 7-Ni. Crystal data are compiled in Table S1 in the Supporting Information. Structures were solved by a heavy metal (7-Pd) and direct (**7**, 7-Ni, and **11**) methods with *SHELXS-97* and refined by a full-matrix least-squares method by using *SHELXL-97* with anisotropic thermal parameters for almost all non-hydrogen atoms. Scattering factors were those incorporated into *SHELXS-97*.[116,117] Electrochemical measurements were performed with an EA9C multifunctional electrochemical analyzer under the following conditions: CH_2Cl_2; 0.1 M TBAP; scan rate, 50 mV s^{-1}; working electrode, glassy carbon disk; auxliary electrode, platinum wire; reference electrode, Ag/AgCl. The voltammograms were referenced against the half-wave potential of Fc/Fc$^+$.

DFT Calculations. Geometry optimizations were carried out within unconstrained C_1 symmetry, with the starting coordinates derived from molecular mechanic calculations.[118] Becke's three-parameter exchange

dx.doi.org/10.1021/ic2027175 | *Inorg. Chem.* 2012, 51, 3247−3260

functional with the gradient-corrected correlation formula of Lee, Yang, and Parr (DFT-B3LYP) was used with the LANL2D basis set for Pd and 6-31G** for other atoms.[119,120] Harmonic vibrational frequencies were calculated using analytical second derivatives. The structure was found to have converged to a minimum on the potential energy surface. The resulting zero-point vibrational energies were included in the calculation of the relative energies. Calculations of the NMR properties for the investigated systems were performed for the optimized structures. Analysis of Wiberg's bond indices was performed for the final geometry using *NBO.3.0* software.[121]

■ ASSOCIATED CONTENT

Supporting Information

Tables of computational results (Cartesian coordinates), figures presenting correlations between calculated and experimental ^{1}H NMR chemical shifts, additional NMR data, cyclic voltammetry data, and X-ray crystallographic data in CIF format. This material is available free of charge *via* the Internet at http://pubs.acs.org.

■ AUTHOR INFORMATION

Corresponding Author

*E-mail: lechoslaw.latos-grazynski@chem.uni.wroc.pl. Tel: +48 71 3757256. Fax: +48 71 3282348. Homepage: http://llg.chem.uni.wroc.pl.

Notes

The authors declare no competing financial interest.

■ ACKNOWLEDGMENTS

Financial support from the Ministry of Science and Higher Education (Grant N N204 013536) is kindly acknowledged. Quantum chemical calculations have been carried out at the Poznań Supercomputer Center (Poznań) and Wrocław Supercomputer Center (Wrocław).

■ REFERENCES

(1) Jux, N.; Koch, P.; Schmickler, H.; Lex, J.; Vogel, E. *Angew. Chem., Int. Ed. Engl.* **1990**, *29*, 1385−1387.
(2) Mártire, D. O.; Jux, N.; Aramendia, P. F.; Negri, R. M.; Lex, J.; Braslavsky, S. E.; Schaffner, K.; Vogel, E. *J. Am. Chem. Soc.* **1992**, *114*, 9969−9978.
(3) Weghorn, S. J.; Lynch, V.; Sessler, J. L. *Tetrahedron Lett.* **1995**, *36*, 4713−4716.
(4) Kurata, H.; Baba, H.; Oda, M. *Chem. Lett.* **1997**, 571−572.
(5) Mena-Osteritz, E.; Bauerle, P. *Adv. Mater.* **2001**, *13*, 243−246.
(6) Fuhrmann, G.; Debaerdemaeker, T.; Bäuerle, P. *Chem. Commun.* **2003**, 948−949.
(7) Kromer, J.; Rios-Carreras, I.; Fuhrmann, G.; Musch, C.; Wunderlin, M.; Debaerdemaeker, T.; Mena-Osteritz, E.; Bauerle, P. *Angew. Chem., Int. Ed.* **2000**, *39*, 3481−3486.
(8) Vogel, E.; Jux, N.; Dorr, J.; Pelster, T.; Berg, T.; Bohm, H. S.; Behrens, F.; Lex, J.; Bremm, D.; Hohlneicher, G. *Angew. Chem., Int. Ed.* **2000**, *39*, 1101−1105.
(9) Berlicka, A.; Latos-Grażyński, L. *Wiad. Chem.* **2008**, *61*, 339−369.
(10) Pawlicki, M.; Latos-Grażyński, L. Carbaporphyrinoids—Synthesis and Coordination Properties. In *Handbook of Porphyrin Science: with Applications to Chemistry, Physics, Materials Science, Engineering, Biology and Medicine*; Kadish, K. M., Smith, K. M., Guilard, R., Eds.; World Scientific Publishing: Singapore, 2010; pp 104−192.
(11) Berlicka, A.; Latos-Grażyński, L.; Lis, T. *Angew. Chem., Int. Ed.* **2005**, *44*, 5288−5291.
(12) Berlicka, A.; Sprutta, N.; Latos-Grażyński, L. *Chem. Commun.* **2006**, 3346−3348.
(13) Meller, A.; Ossko, A. *Monatsh. Chem.* **1972**, *103*, 150−155.
(14) Rodriguez-Morgade, M. S.; Esperanza, S.; Torres, T.; Barbera, J. *Chem.—Eur. J.* **2004**, *11*, 354−360.
(15) Inokuma, Y.; Kwon, J. H.; Ahn, T. K.; Yoo, M. C.; Kim, D.; Osuka, A. *Angew. Chem., Int. Ed.* **2006**, *45*, 961−964.
(16) Inokuma, Y.; Yoon, Z. S.; Kim, D.; Osuka, A. *J. Am. Chem. Soc.* **2007**, *129*, 4747−4761.
(17) Takeuchi, Y.; Matsuda, A.; Kobayashi, N. *J. Am. Chem. Soc.* **2007**, *129*, 8271−8281.
(18) Myśliborski, R.; Latos-Grażyński, L.; Szterenberg, L.; Lis, T. *Angew. Chem., Int. Ed.* **2006**, *45*, 3670−3674.
(19) Heremans, P.; Cheyns, D.; Rand, B. P. *Acc. Chem. Res.* **2009**, *42*, 1740−1747.
(20) Torres, T. *Angew. Chem., Int. Ed.* **2006**, *45*, 2834−2837.
(21) Claessens, C. G.; Gonzalez-Rodriguez, D.; Torres, T. *Chem. Rev.* **2002**, *102*, 835−853.
(22) Rodriguez, D.; Torres, T.; Guldi, D. M.; Rivera, J.; Herranz, M. A.; Echegoyen, L. *J. Am. Chem. Soc.* **2004**, *126*, 6301−6313.
(23) Kobayashi, N. Synthesis and Spectroscopic Properties of Phthalocyanine Analogs. In *The Porphyrin Handbook*; Kadish, K. M., Smith, K. M., Guilard, R., Eds.; Academic Press: San Diego, 2003; pp 161−162.
(24) Inokuma, Y.; Osuka, A. *Dalton Trans.* **2008**, 2517−2526.
(25) Anju, K. S.; Ramakrishnan, S.; Srinivasan, A. *Org. Lett.* **2011**, *13*, 2498−2501.
(26) Xue, Z. L.; Mack, J.; Lu, H.; Zhang, L.; You, X. Z.; Kuzuhara, D.; Stillman, M.; Yamada, H.; Yamauchi, S.; Kobayashi, N.; Shen, Z. *Chem.—Eur. J.* **2011**, *17*, 4396−4407.
(27) Kuzuhara, D.; Yamada, H.; Xue, Z. L.; Okujima, T.; Mori, S.; Shen, Z.; Uno, H. *Chem. Commun.* **2011**, *47*, 722−724.
(28) Xue, Z. L.; Shen, Z.; Mack, J.; Kuzuhara, D.; Yamada, H.; Okujima, T.; Ono, N.; You, X. Z.; Kobayashi, N. *J. Am. Chem. Soc.* **2008**, *130*, 16478.
(29) Badger, G. M.; Elix, J. A.; Lewis, G. E. *Aust. J. Chem.* **1965**, *18*, 70−89.
(30) Badger, G. M.; Elix, J. A.; Lewis, G. E. *Aust. J. Chem.* **1966**, *19*, 1220−1241.
(31) Badger, G. M.; Lewis, G. E.; Singh, U. P. *Aust. J. Chem.* **1967**, *20*, 1635−1642.
(32) Pacholska, E.; Latos-Grażyński, L.; Ciunik, Z. *Chem.—Eur. J.* **2002**, *8*, 5403−5406.
(33) Pacholska-Dudziak, E.; Skonieczny, J.; Pawlicki, M.; Szterenberg, L.; Ciunik, Z.; Latos-Grażyński, L. *J. Am. Chem. Soc.* **2008**, *130*, 6182−6195.
(34) Pacholska-Dudziak, E.; Gaworek, A.; Latos-Grażyński, L. *Inorg. Chem.* **2011**, *50*, 10956−10965.
(35) Pawlicki, M.; Latos-Grażyński, L. *Chem. Rec.* **2006**, *6*, 64−78.
(36) Krupowicz, J.; Sapiecha, K. *Rocz. Chem.* **1973**, *47*, 1729−1730.
(37) Krupowicz, J.; Sapiecha, K.; Gaszczyk, R. *Rocz. Chem.* **1974**, *48*, 2067−2068.
(38) Lockwood, R. F.; Nicholas, K. M. *Tetrahedron Lett.* **1977**, 4163−4166.
(39) Padmanabhan, S.; Nicholas, K. M. *Tetrahedron Lett.* **1983**, *24*, 2239−2242.
(40) Schreiber, S. L.; Klimas, M. T.; Sammakia, T. *J. Am. Chem. Soc.* **1987**, *109*, 5749−5759.
(41) Nicholas, K. M. *Acc. Chem. Res.* **1987**, *20*, 207−214.
(42) Teobald, B. J. *Tetrahedron* **2002**, *58*, 4133−4170.
(43) Omae, I. *Appl. Organomet. Chem.* **2007**, *21*, 318−344.
(44) Bromfield, K. M.; Graden, H.; Ljungdahl, N.; Kann, N. *Dalton Trans.* **2009**, 5051−5061.
(45) Lash, T. D. *Eur. J. Org. Chem.* **2007**, 5461−5481.
(46) Stępień, M.; Latos-Grażyński, L. *J. Am. Chem. Soc.* **2002**, *124*, 3838−3839.
(47) Stępień, M.; Latos-Grażyński, L.; Szterenberg, L.; Panek, J.; Latajka, Z. *J. Am. Chem. Soc.* **2004**, *126*, 4566−4580.
(48) Szyszko, B.; Latos-Grażyński, L. *Organometallics* **2011**, *30*, 4354−4363.
(49) Stępień, M.; Szyszko, B.; Latos-Grażyński, L. *Org. Lett.* **2009**, *11*, 3930−3933.
(50) Hung, C. H.; Lin, C. Y.; Lin, P. Y.; Chen, Y. J. *Tetrahedron Lett.* **2004**, *45*, 129−132.

(51) Latos-Grażyński, L.; Lisowski, J.; Olmstead, M. M.; Balch, A. L. *J. Am. Chem. Soc.* **1987**, *109*, 4428−4429.
(52) Kawase, T.; Muro, S.; Kurata, H.; Oda, M. *J. Chem. Soc., Chem. Commun.* **1992**, 778−779.
(53) Vandonge, J. P.; Debie, M. J. A.; Steur, R. *Tetrahedron Lett.* **1973**, 1371−1374.
(54) Nakagawa, M. *Angew. Chem., Int. Ed. Engl.* **1979**, *18*, 202−214.
(55) Stępień, M.; Latos-Grażyński, L. Aromaticity and tautomerism in porphyrins and porphyrinoids. In *Aromaticity in Heterocyclic Compounds*; Krygowski, T. M., Ed.; Springer: Berlin/Heidelberg, 2009; pp 83−154.
(56) Vogel, E.; Röhrig, P.; Sicken, M.; Knipp, B.; Herrmann, A.; Pohl, M.; Schmickler, H.; Lex, J. *Angew. Chem., Int. Ed. Engl.* **1989**, *28*, 1651−1655.
(57) Stępień, M.; Latos-Grażyński, L. *Chem.—Eur. J.* **2001**, *7*, 5113−5117.
(58) Skonieczny, J.; Latos-Grażyński, L.; Szterenberg, L. *Chem.—Eur. J.* **2008**, 4861−4874.
(59) Nervi, C.; Gobetto, R.; Milone, L.; Viale, A.; Rosenberg, E.; Rokhsana, D.; Fiedler, J. *Chem.—Eur. J.* **2003**, *9*, 5749−5756.
(60) Myśliborski, R.; Latos-Grażyński, L.; Szterenberg, L. *Eur. J. Org. Chem.* **2006**, 3064−3068.
(61) Chmielewski, P. J.; Latos-Grażyński, L. *Inorg. Chem.* **1992**, *31*, 5231−5235.
(62) Lisowski, J.; Latos-Grażyński, L.; Szterenberg, L. *Inorg. Chem.* **1992**, *31*, 1933−1940.
(63) Latos-Grażyński, L. Core Modified Heteroanalogues of Porphyrins and Metalloporphyrins. In *The Porphyrin Handbook*; Kadish, K. M., Smith, K. M., Guilard, R., Eds.; Academic Press: New York, 2000; pp 361−416.
(64) Pacholska-Dudziak, E.; Latos-Grażyński, L. *Eur. J. Inorg. Chem.* **2007**, 2594−2608.
(65) Ram, M. S.; Riordan, C. G.; Yap, G. P. A.; Liables-Sands, L.; Rheingold, A. L.; Marchaj, A.; Norton, J. R. *J. Am. Chem. Soc.* **1997**, *119*, 1648.
(66) Kläui, W.; Huhn, M.; Herbst-Irmer, R. *J. Organomet. Chem.* **1991**, *415*, 133−142.
(67) Chmielewski, P. J.; Latos-Grażyński, L.; Głowiak, T. *J. Am. Chem. Soc.* **1996**, *118*, 5690−5701.
(68) Latos-Grażyński, L.; Lisowski, J.; Chmielewski, P. J.; Grzeszczuk, M.; Olmstead, M. M.; Balch, A. L. *Inorg. Chem.* **1994**, *33*, 192−197.
(69) Szyszko, B.; Latos-Grażyński, L.; Szterenberg, L. *Angew. Chem., Int. Ed.* **2011**, *50*, 6587−6591.
(70) Bondi, A. *J. Phys. Chem.* **1964**, *68*, 441−451.
(71) Hahn, C.; Vitagliano, A.; Giordano, F.; Taube, R. *Organometallics* **1998**, *17*, 2060−2066.
(72) Rettig, M. F.; Wing, R. M.; Wiger, G. R. *J. Am. Chem. Soc.* **1981**, *103*, 2980−2986.
(73) Ghebreyessus, K. Y.; Ellern, A.; Angelici, R. J. *Organometallics* **2005**, *24*, 1725−1736.
(74) Miki, K.; Shiotani, O.; Kai, Y.; Kasai, N.; Kanatani, H.; Kurosawa, H. *Organometallics* **1983**, *2*, 585−593.
(75) Smith, D. E.; Welch, A. J. *Acta Crystallogr., Sect. C* **1986**, *42*, 1717−1720.
(76) Orpen, A. G.; Brammer, L.; Allen, F. H.; Kennard, O.; Watson, D. G.; Taylor, R. *J. Chem. Soc., Dalton Trans.* **1989**, S1−S83.
(77) Binotti, B.; Bellachioma, G.; Cardaci, G.; Macchioni, A.; Zuccaccia, C.; Foresti, E.; Sabatino, P. *Organometallics* **2002**, *21*, 346−354.
(78) Klein, A.; Luening, A.; Ott, I.; Hamel, L.; Neugebauer, M.; Butsch, K.; Lingen, V.; Heinrich, F.; Elmas, S. *J. Organomet. Chem.* **2010**, *695*, 1898−1905.
(79) Kang, M.; Sen, A. *Organometallics* **2004**, *23*, 5396−5398.
(80) Meinhard, D.; Hollmann, F.; Huhn, W.; Thewalt, U.; Klinga, M.; Rieger, B. *Organometallics* **2004**, *23*, 5637−5639.
(81) Ciajolo, R.; Jama, M. A.; Tuzi, A.; Vitagliano, A. *J. Organomet. Chem.* **1985**, *295*, 233−238.
(82) Berenguer, J. R.; Fornies, J.; Lalinde, E.; Martinez, F. *Organometallics* **1996**, *15*, 4537−4546.
(83) Ara, I.; Falvello, L. R.; Fernandez, S.; Fornies, J.; Lalinde, E.; Martin, A.; Moreno, M. T. *Organometallics* **1997**, *16*, 5923−5937.
(84) Pla-Quintana, A.; Torrent, A.; Dachs, A.; Roglans, A.; Pleixats, R.; Moreno-Manas, M.; Parella, T.; Benet-Buchholz, J. *Organometallics* **2006**, *25*, 5612−5620.
(85) Battiste, M. A.; Griggs, B. G.; Sackett, D.; Coxon, J. M.; Steel, P. J. *J. Organomet. Chem.* **1987**, *330*, 437−446.
(86) Churchil, M. R.; Deboer, B. G.; Hackbart, J. J. *Inorg. Chem.* **1974**, *13*, 2098−2105.
(87) Li, X. Y.; Sun, H. J.; Florke, U.; Klein, H. F. *Organometallics* **2005**, *24*, 4347−4350.
(88) Taube, R.; Langlotz, J.; Sieler, J.; Gelbrich, T.; Tittes, K. *J. Organomet. Chem.* **2000**, *597*, 92−104.
(89) O'Connor, A. R.; White, P. S.; Brookhart, M. *J. Am. Chem. Soc.* **2007**, *129*, 4142−4143.
(90) Bach, I.; Porschke, K. R.; Proft, B.; Goddard, R.; Kopiske, C.; Kruger, C.; Rufinska, A.; Seevogel, K. *J. Am. Chem. Soc.* **1997**, *119*, 3773−3781.
(91) Bach, I.; Porschke, K. R.; Goddard, R.; Kopiske, C.; Kruger, C.; Rufinska, A.; Seevogel, K. *Organometallics* **1996**, *15*, 4959−4966.
(92) Pulst, S.; Arndt, P.; Heller, B.; Baumann, W.; Kempe, R.; Rosenthal, U. *Angew. Chem., Int. Ed. Engl.* **1996**, *35*, 1112−1115.
(93) Bennett, M. A.; Johnson, J. A.; Willis, A. C. *Organometallics* **1996**, *15*, 68−74.
(94) Edelbach, B. L.; Lachicotte, R. J.; Jones, W. D. *Organometallics* **1999**, *18*, 4660−4668.
(95) Latos-Grażyński, L.; Olmstead, M. M.; Balch, A. L. *Inorg. Chem.* **1989**, *28*, 4065−4066.
(96) Latos-Grażyński, L.; Lisowski, J.; Olmstead, M. M.; Balch, A. L. *Inorg. Chem.* **1989**, *28*, 1183−1188.
(97) Pohl, M.; Schmickler, H.; Lex, J.; Vogel, E. *Angew. Chem., Int. Ed. Engl.* **1991**, *30*, 1693−1697.
(98) Cissell, J. A.; Vaid, T. P.; Rheingold, A. L. *J. Am. Chem. Soc.* **2005**, *127*, 12212−12213.
(99) Cissell, J. A.; Vaid, T. P.; Yap, G. P. A. *Org. Lett.* **2006**, *8*, 2401−2404.
(100) Cissell, J. A.; Vaid, T. P.; Yap, G. P. A. *J. Am. Chem. Soc.* **2007**, *129*, 7841−7847.
(101) Yamamoto, Y.; Yakamoto, A.; Furuta, S.; Horie, M.; Kodama, M.; Satao, W.; Akiba, K.; Tsuzuki, S.; Uchimaru, T.; Hashizume, D.; Iwasaki, F. *J. Am. Chem. Soc.* **2005**, *127*, 14540−14541.
(102) Yamamoto, Y.; Hirata, Y.; Kodama, M.; Yamaguchi, T.; Matsukawa, S.; Akiba, K. y.; Hashizume, D.; Iwasaki, F.; Muranaka, A.; Uchiyama, M.; Chen, P.; Kadish, K. M.; Kobayashi, N. *J. Am. Chem. Soc.* **2010**, *132*, 12627−12638.
(103) Wiberg, K. B. *Tetrahedron* **1968**, *24*, 1083−1096.
(104) Chen, Z.; Wannere, C. S.; Corminboeuf, C.; Puchta, R.; Schleyer, P. *Chem. Rev.* **2005**, *105*, 3842−3888.
(105) Schleyer, P.; Meaerker, C.; Dransfeld, A.; Jiao, H.; Hommes, N. J. R. *J. Am. Chem. Soc.* **1996**, *118*, 6317−6318.
(106) Cyrański, M. K.; Krygowski, T. M.; Wisiorowski, M.; Hommes, N. J. R.; Schleyer, P. *Angew. Chem., Int. Ed. Engl.* **1998**, *37*, 177−180.
(107) Juselius, J.; Sundholm, D. *J. Org. Chem.* **2000**, *65*, 5233−5237.
(108) Simkowa, I.; Latos-Grażyński, L.; Stępień, M. *Angew. Chem., Int. Ed.* **2010**, *49*, 7665−7669.
(109) Stępień, M.; Latos-Grażyński, L.; Szterenberg, L. *J. Org. Chem.* **2007**, *72*, 2259−2270.
(110) Furuta, H.; Maeda, H.; Osuka, A. *J. Org. Chem.* **2001**, *66*, 8563−8572.
(111) Toganoh, M.; Furuta, H. *J. Org. Chem.* **2010**, *75*, 8213−8223.
(112) Castro, C.; Isborn, C. M.; Karney, W. L.; Mauksch, M.; Schleyer, P. *Org. Lett.* **2002**, *4*, 3431−3434.
(113) Pacholska-Dudziak, E.; Skonieczny, J.; Pawlicki, M.; Latos-Grażyński, L.; Szterenberg, L. *Inorg. Chem.* **2005**, *44*, 8794−8803.
(114) Pacholska-Dudziak, E.; Latos-Grażyński, L. *Coord. Chem. Rev.* **2009**, *253*, 236−248.
(115) Ulman, A.; Manassen, J. *J. Chem. Soc., Perkin Trans. 1* **1979**, 1066−1069.

(116) *SHELXL97—Program for Crystal Structure Refinement*; University of Göttingen: Göttingen, Germany, 1997.
(117) *SHELXS97—Program for Crystal Structure Solution*; University of Göttingen: Göttingen, Germany, 1997.
(118) Frisch, M. J.; Trucks, G. W.; Schlegel, H. B.; Scuseria, G. E.; Robb, M. A.; Cheeseman, J. R.; Scalmani, G.; Barone, V.; Mennucci, B.; Petersson, G. A.; Nakatsuji, H.; Caricato, M.; Li, X.; Hratchian, H. P.; Izmaylov, A. F.; Bloino, J.; Zheng, G.; Sonnenberg, J. L.; Hada, M.; Ehara, M.; Toyota, K.; Fukuda, R.; Hasegawa, J.; Ishida, M.; Nakajima, T.; Honda, Y.; Kitao, O.; Nakai, H.; Vreven, T.; Montgomery, J. A., Jr.; Peralta, J. E.; Ogliaro, F.; Bearpark, M.; Heyd, J. J.; Brothers, E.; Kudin, K. N.; Staroverov, V. N.; Kobayashi, R.; Normand, J.; Raghavachari, K.; Rendell, A.; Burant, J. C.; Iyengar, S. S.; Tomasi, J.; Cossi, M.; Rega, N.; Millam, N. J.; Klene, M.; Knox, J. E.; Cross, J. B.; Bakken, V.; Adamo, C.; Jaramillo, J.; Gomperts, R.; Stratmann, R. E.; Yazyev, O.; Austin, A. J.; Cammi, R.; Pomelli, C.; Ochterski, J. W.; Martin, R. L.; Morokuma, K.; Zakrzewski, V. G.; Voth, G. A.; Salvador, P.; Dannenberg, J. J.; Dapprich, S.; Daniels, A. D.; Farkas, Ö.; Foresman, J. B.; Ortiz, J. V.; Cioslowski, J.; Fox, D. J. *Gaussian 09*, revision A.1; Gaussian, Inc.: Wallingford, CT, 2009.
(119) Lee, C.; Yang, W.; Parr, R. G. *Phys. Rev. B* **1988**, *37*, 785−789.
(120) Becke, A. D. *Phys. Rev. A* **1988**, *38*, 3098−3100.
(121) Glendening, E. D.; Reed, A. E.; Carpenter, I. J.; Weinhold, F. *The NBO3.0 program*; University of Wisconsin: Madison, MI, 1996.